NATIONAL ADVISORY COMMITTEE FOR AERONAUTICS

TECHNICAL NOTE

No. 1826

LINEAR THEORY OF BOUNDARY EFFECTS IN OPEN

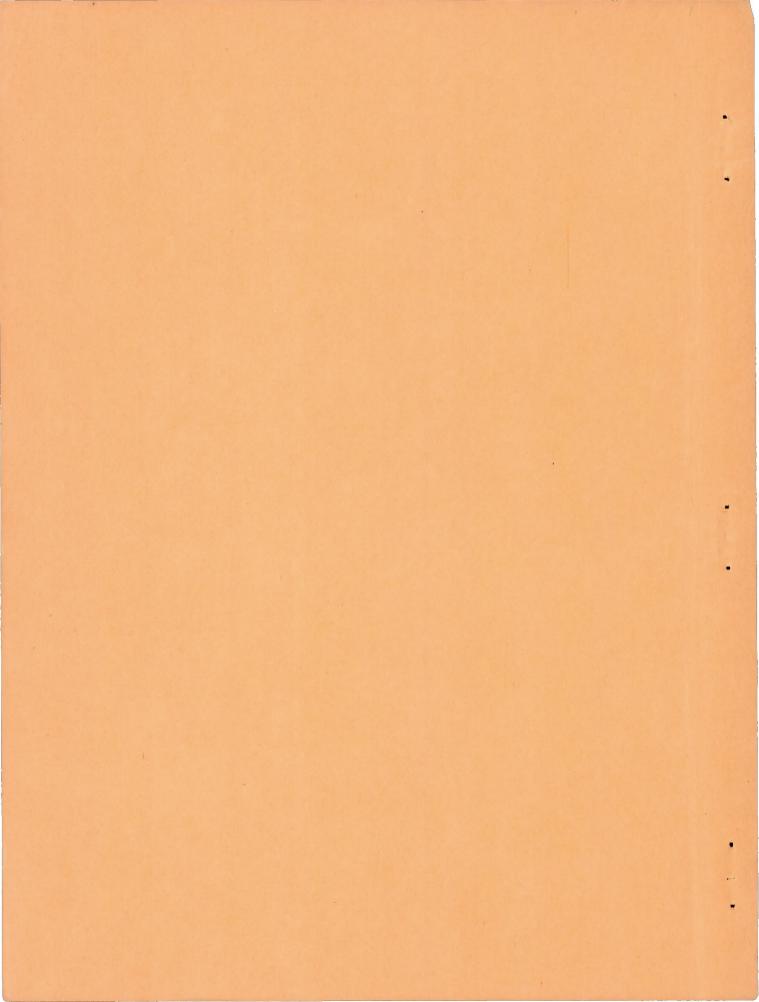
WIND TUNNELS WITH FINITE JET LENGTH

By S. Katzoff, Clifford S. Gardner, Leo Diesendruck, and Bertram J. Eisenstadt

> Langley Aeronautical Laboratory Langley Air Force Base, Va.



Washington March 1949



NATIONAL ADVISORY COMMITTEE FOR AERONAUTICS

TECHNICAL NOTE No. 1826

LINEAR THEORY OF BOUNDARY EFFECTS IN OPEN

WIND TUNNELS WITH FINITE JET LENGTH

By S. Katzoff, Clifford S. Gardner, Leo Diesendruck, and Bertram J. Eisenstadt

SUMMARY

In the first part, the boundary conditions for an open wind tunnel (incompressible flow) are examined with special reference to the effects of the closed entrance and exit sections. Basic conditions are that the velocity must be continuous at the entrance lip and that the velocities in the upstream and downstream closed portions must be equal. For the two-dimensional open tunnel, interesting possibilities develop from the fact that the pressures on the two free surfaces need not be equal.

Electrical analogies that might be used for solving the flow in open wind tunnels are outlined. Two types are described - one in which electrical potential corresponds to velocity potential, and another in which electrical potential corresponds to acceleration potential. The acceleration-potential analogies are probably experimentally simpler than the velocity-potential analogies.

In the second part, solutions are derived for four types of twodimensional open tunnels, including one in which the pressures on the two free surfaces are not equal. Numerical results are given for every case. In general, if the lifting element is more than half the tunnel height from the inlet, the boundary effect at the lifting element is the same as for an infinitely long open tunnel.

In the third part is given a general method for calculating the boundary effect in an open circular wind tunnel of finite jet length. Numerical results are given for a lifting element concentrated at a point on the axis.

INTRODUCTION

The basic theory of boundary corrections for an open wind tunnel was given by Prandtl many years ago (reference 1) and has since been used with reasonable success. The infinitely long open jet that was assumed in Prandtl's analysis, however, has been frequently questioned as an adequate representation for an open wind tunnel, which normally has a relatively short jet between closed entrance and exit regions.

The present examination of the problem was occasioned by the need for boundary corrections for tests in the Langley full-scale tunnel of a large helicopter, of which the forward edge of the rotor disk reached almost to the mouth of the entrance bell while the rear edge approached the exit bell. Previous studies (reference 2) had shown that the Prandtl theory was satisfactory for a wing in the usual position in the tunnel (about 20 feet downstream of the entrance); but it was felt that this simple theory was inadequate for such far forward and rearward locations of the lifting surface, and that some further development was desirable. The only previous analysis bearing directly on the problem seemed to be that of reference 3, which considered a lifting element concentrated at a point on the axis of a circular open tunnel of finite jet length; however, the treatment therein was not rigorous, and was justified only by a somewhat heuristic discussion, so that its general applicability was not obvious. Other studies treated either twodimensional or axially symmetrical conditions (references 4 and 5) and also did not consider the closed exit region, so that the extent of their applicability to the present problem was not at first apparent. A similar German wartime report (reference 6), which did not become available until after the present paper was written, would have been more useful in this respect because of the generality of its physical discussion.

Because of the particular shape of the tunnel cross section, a reasonably simple solution in terms of available functions seemed unlikely; accordingly, the initial effort was directed toward defining the problem in such a way that it could be solved by analogy methods in an electrical tank. Identification of the necessary boundary conditions appeared at first to be somewhat perplexing; however, after recognition of some of the basic physical phenomena, the boundary conditions were readily clarified. The problem is thus considered now to be fairly well understood, at least insofar as it can be considered linear and uninfluenced by turbulent mixing at the free surfaces or by the irregular nature of the flow at the exit. As will appear later, however, grave technical difficulties exist in the exact solution by electrical-analogy methods, so that, for example, actual evaluation of the tunnel interference for the large helicopter in the Langley full-scale tunnel, which problem instigated the present research, has not yet been accomplished.

After the boundary conditions were clarified, analytical methods of solution were developed for two-dimensional and circular open tunnels. These studies have been combined with the discussion of the boundary conditions and the electrical analogies to form the present paper, which, it is hoped, will serve to clarify basic concepts and establish a sound basis for any further work.

The report is divided into three parts. In part I, the boundary conditions are defined and discussed for the open wind tunnel with closed entrance and exit sections, and an outline is given of suggested electrical analogies applicable to the problem. In part II, analytical solutions are given for various two-dimensional open-tunnel types,

NACA TN No. 1826

together with numerous calculated results. In part III, a method of solution for the circular open tunnel is given, together with numerical results for the case of a lifting element concentrated at a point on the axis of the tunnel. The treatment in every case is a linear one in which deformation of the jet boundary is considered to be small.

The parts were essentially independently prepared. Messrs. Gardner and Diesendruck contributed the analysis of part II. Mr. Eisenstadt contributed part III. Dr. Katzoff contributed part I, and, in the absence of the others, prepared the numerical results of part II, made several minor revisions, and served as general editor of the whole.

I - BOUNDARY CONDITIONS AND

ELECTRICAL ANALOGIES

In part I, boundary conditions for an open wind tunnel are discussed with special reference to the effects of the closed entrance and exit sections. It is shown that the velocity on the free surface is not necessarily equal to the velocity far upstream in the closed portion and that cross-flows may exist in the free surface, unlike the case of the infinitely long open jet. A basic condition - analogous to the Kutta-Joukowski condition for the flow at the trailing edge of an airfoil - is that the velocity be continuous at the entrance lip. Electrical analogies that might be used for solving the flow in open wind tunnels are outlined. Two types are described - one in which electrical potential corresponds to velocity potential, and another in which electrical potential corresponds to acceleration potential.

BOUNDARY CONDITIONS

Résumé of Prandtl's theory. In Prandtl's original discussion, in which the entrance and exit regions are neglected, the tunnel is considered as an infinitely long cylinder on the entire surface of which the pressure is constant, whence, by Bernoulli's law, the velocity on the surface is constant. If this velocity is considered as the sum of the undisturbed tunnel velocity U and a small perturbation velocity (u,v,w) due to the presence of a body in the jet, the condition is then that $(U+u)^2+v^2+w^2\approx U^2+2Uu=\text{Constant}$, from which it is concluded that u is constant over the entire surface. Furthermore, since u is obviously zero far in front of the body, it must be zero over the entire surface.

A corollary is that, on the jet surface, the perturbation velocity normal to u (that is, the circumferential velocity) is also zero, as is readily shown from a consideration of the rectangular path SPQR on the surface of the jet. (See fig. 1(a).) As has just been shown, the

velocity component u parallel to the lines SP and QR is zero; hence, the perturbation potentials at points P and Q are the same as at points S and R, respectively. If points S and R are far upstream of the body their potentials will be equal, so that the potentials at points P and Q are equal. The perturbation potential is thus uniform over the entire surface, and only perturbation velocities normal to the surface can exist at the surface.

Modification of basic concepts - If the closed entrance region is near the body, as shown in figure 1(b), the preceding discussion and conclusions no longer apply. Thus, although u must still be constant over the entire free surface, it is no longer necessarily zero; that is, the total velocity on the free surface is not necessarily equal to the velocity far upstream in the closed portion of the tunnel. The two velocities will, in fact, generally be unequal except in special cases where equality results from geometrical symmetry of the arrangement. (For example, if a horseshoe vortex is located in the horizontal plane of symmetry of the tunnel, the values of u at the top and bottom of the tunnel would be expected to be equal and opposite; but since u must be uniform over the surface, it follows that u = 0.) Furthermore, the velocities in the jet surface normal to u (that is, the circumferential velocities) are, in general, no longer zero (except for axially symmetrical flows, such as that produced by a source on the axis of a circular tunnel) so that two surface points at the same longitudinal position, as P' and Q' (fig. 1(b)) do not necessarily have the same values of the perturbation potential.

Entrance-lip condition -- Consider, for simplicity, the symmetrical case of figure 1(b), in which the lifting element is on the horizontal plane of symmetry of the tunnel. Since u is zero on the free boundary, the perturbation potential is constant along the elements AB, CD, EF, . . ., although, as just indicated, it is not necessarily the same for all these elements. This one boundary condition for the open section that the potential be constant along each of these elements - does not suffice, however, to define the problem uniquely. In fact, as will be obvious from the subsequent discussion of electrical analogies, the potentials of these elements may be quite arbitrarily assigned without violating this condition or the boundary condition on the closed portion of the tunnel (that the normal derivative of the potential be zero at the wall). In order to avoid this lack of uniqueness, further conditions must be sought. The most important of these is that the velocity be continuous (in particular, not infinite) at the entrance lip (points A, C, E. . . .). This condition takes cognizance of the fact that, because of viscosity, the physical flow leaves the lip smoothly, just as it leaves the trailing edge of an airfoil; the condition is, in fact, strictly analogous to the Kutta-Joukowski condition for the trailing-edge of an airfoil, which similarly takes into account the basic viscosity effect and provides uniqueness where otherwise an infinity of solutions would exist. It is recognized that, just as the Kutta-Joukowski condition does not always suffice to predict airfoil lift very accurately, the corresponding condition for the open tunnel may similarly oversimplify the entrance-lip

flow; however, as with the airfoil, the condition is probably adequate where the flow is not subject to an excessive pressure rise on approaching the lip. References 4, 5, and 6 used the condition, and reference 6, in addition, discussed it from the physical viewpoint and compared it with the airfoil trailing-edge condition.

Concerning the downstream end of the open section, the exit lip may be considered to correspond to the leading edge of an airfoil and no effort need be made in an idealized flow analysis to eliminate infinite values of u at this edge.

Jet contraction or expansion. It has already been pointed out that, with a body in the jet, the velocity on the free surface is not necessarily equal to the velocity far upstream in the closed portion. During the course of the investigation, it was noted that solutions could be obtained showing a difference between these two velocities, even when there was no body in the jet. Such a flow corresponds merely to a contraction or expansion of the jet, as indicated in figure 2. Thus, in figure 2(a), the velocity on the free surface is lower than the upstream velocity and remains so even as it approaches the exit, in spite of the gradual contraction of the jet, because of the continuously increasing surface curvature. The velocity suddenly increases at the exit lip and finally is established at a value greater than that of the upstream velocity. With reasonable ratios of entrance to exit area, the flows of figure 2 may be readily obtained experimentally.

The significance of this expanding or contracting flow is that it represents a solution that satisfies all the boundary conditions previously discussed and is nevertheless undesirable. In order to avoid such solutions, a further condition must accordingly be recognized; namely, that the velocities in the closed portions far upstream and far downstream of the open section be equal.

It may be objected that in the normal design of an open wind tunnel the exit section is made larger than the entrance section. The purpose of the increased area is to allow for the reduced velocity toward the surface of the jet resulting from turbulent mixing with the surrounding still air. Increasing the exit area by other than the correct amount will result in the type of flow indicated in figures 2(a) or 2(b), with a corresponding velocity gradient along the center of the tunnel. In any potential-flow solution these viscous effects cannot be considered.

Spillage. When an airfoil is tested at a high lift coefficient in an open tunnel, the downward deflection of the jet may result in appreciable spillage from the lower lip of the exit, together with lack of contact of the main flow with the upper lip. (See fig. 3(a).) The air lost by spillage is replaced by air (of, however, a lower total pressure) entrained in the exit. Even without otherwise considering the distortion of the free surface, these flow characteristics might seem too much at variance with the previously assumed characteristics to permit application of the theories being discussed. The calculations of part II for

the two-dimensional open tunnel (that is, a rectangular tunnel with closed sides but open top and bottom) show, however, very little difference between the tunnel-induced-downwash distributions for the tunnel with two exit lips and the tunnel with one exit lip. That is, if figure 3(a) is assumed to represent a two-dimensional flow, the fact that the upper lip of the exit is out of the flow field so that the lower lip takes over the entire burden of straightening the jet does not greatly affect the induced downwash.

The effect of the exit lip on the flow phenomena is the least clear of the various phases of the present problem. For open wind tunnels having essentially unflared exits, similar to that indicated in figure 3(a), the suggestions of the preceding paragraph are probably adequate. The exit of the Langley full-scale tunnel, however, has a large bell mouth, and when airplanes are being tested at high lift coefficients a downward deflection of the air off the lower part of the bell, roughly as indicated in figure 3(b), occurs. Whether the previously suggested concepts or, indeed, any linear theory can serve satisfactorily for this case seems questionable.

Unequal surface pressures. An interesting method of avoiding spillage suggests itself in the case of the two-dimensional open tunnel: If the space below the tunnel is inclosed, an excess pressure will be built up in this space, compared with the pressure in the space above the upper free surface, so that the flow will be pushed up sufficiently to eliminate the spillage and ensure precise contact of the lower free surface with the lower exit lip. (See fig. 3(c).) The extent to which a free two-dimensional jet can be deformed by a pressure difference across its boundaries, or, stated differently, the extent to which a two-dimensional free jet will deform in order to follow the only available path, is indicated by the smoke-flow photograph in figure 4. The setup consisted merely of a two-dimensional open jet with entrance and exit sections displaced vertically relative to each other, arranged between transparent side walls, and provided with enclosed spaces above and below.

Details of interest in the figure, in addition to the jet deformation, are:

- (1) Separation of the flow from the upper lip of the exit, because of the large angle of entry. A small bell mouth at the exit lip might have prevented such separation.
- (2) The rough flow on the upper surface at the entrance, compared with the smooth flow on the lower surface, reflects the fact that the boundary layer approaching the entrance is subjected to a rising pressure on the upper surface and a dropping pressure on the lower surface.
- (3) Because of turbulent mixing at the free surfaces, a certain amount of the air in the closed chambers above and below the jet is entrained in the jet. An equivalent quantity must be released, or skimmed off, at the exit in order that the total quantity in each chamber

remain constant. This circulating mechanism results in the apparent overflow at the two exit lips. The return of the skimmed-off part to the jet surface can be seen at the bottom of the photograph.

Tunnel without a closed exit. Some mention is made in the subsequent discussion of the hypothetical open tunnel having a closed upstream entrance region but no closed exit region, the open section thus extending downstream to infinity. Calculations for such an arrangement (see part II) are generally simpler than for the actual tunnel with the closed exit, and give very nearly the same answer, provided that the region of interest is much closer to the entrance than to the exit, as is usually the case. For this arrangement, solutions with an arbitrary contraction or expansion of the jet cannot exist, so that no effort need be made to avoid them. The solution for the general unsymmetrical case, however, will show the jet velocity downstream at infinity to be different from the velocity upstream in the closed part. The possibility that, in the two-dimensional case, different pressures might be assumed on the two free surfaces still exists for this type of tunnel, but the resulting jet will have a constant curvature after leaving the neighborhood of the body.

An upstream condition for the "infinitely long" open tunnel and a correction to the results of reference 8. In many discussions of the two-dimensional open tunnel, the set of images indicated in figure 5(a) is used to satisfy the boundary condition that u = 0, and the resulting flow shows an upflow in front and an equal downflow in back, with no induced downwash at the wing itself. Actually, however, if the jet issues from a horizontal closed entrance - no matter how far upstream - it will remain essentially horizontal (because it is not subjected to any vertical force) until it reaches the wing. (See fig. 5(b).) In order to eliminate the undesired upstream upwash, a uniform downwash should therefore be added to the solution indicated in figure 5(a). (compare reference 7, p. 304.) Addition of this downwash does not affect the boundary conditions, since u is still zero at the boundary. This case is discussed quantitatively in part II, where it is shown that the entrance-lip condition automatically provides the correct answer.

Among the rectangular wind tunnels for which corrections were given in reference 8 is a type with closed sides but open top and bottom. The calculated corrections for approximately square cross sections are approximately equal to those for the completely closed tunnel, a surprising result in view of the absence of any top or bottom constraint. The result is actually in error, as was discovered in an experimental effort to verify it (reference 9). In seeking to explain the errors the author of reference 9 pointed out that the image system used in reference 8 should have included an infinite row of vortices at infinity, and he showed how, by taking into account this row of vortices, the correct answer could be obtained. It could not be shown, however, that the extent of this row of vortices is of a higher order of infinity than is their distance from the origin, as is necessary if their effect is to be considered. The method of the preceding paragraph thus appears to be much simpler and more rigorous in such cases than is a discussion of the image vortices at infinity. One simply observes that the image system

of reference 8 provides an angle correction factor δ of 0.25 for the flow far upstream of the wing, whereas δ should be zero far upstream; a correction of -0.25 should therefore be added to all values of δ computed by this image system for points within the tunnel.

Summary of boundary conditions. A basic physical characteristic of the flow is provided by the condition that the velocity be continuous at the entrance lip, which also helps to provide uniqueness. The velocity on the free surface is not necessarily the velocity far upstream in the closed portion; in fact, for the two-dimensional case, it is even possible for the pressures on the two free surfaces to be different from each other. Equality of the velocities in the upstream and downstream closed portions has been recognized as an additional condition. Neglecting the upper portion of the closed exit may be desirable if the flow is so depressed that it does not make contact with the upper part of the exit. Neglecting the entire closed exit region may appreciably simplify the problem without introducing excessive inaccuracy if the region of interest is much closer to the entrance than to the exit. In general, adequate treatment of the exit (for large lift on the body in the tunnel) seems very unlikely.

The discussion in the preceding sections has concerned mainly the physical flow conditions, and relatively little interpretation in terms of boundary conditions on the perturbation potential has been given, although such formal interpretation would appear a trivial task. The reason that this extension has not been made is that, in a number of instances, as will appear subsequently, slight modifications of the basic viewpoint, leading to somewhat modified boundary conditions, are desirable for convenience of solution. Accordingly, the statements of the boundary conditions on the perturbation potentials will be given when the solutions are discussed.

SUGGESTED ELECTRICAL ANALOGIES

Velocity-Potential Analogies

Basic concepts of the analogies. In the analogies to be discussed in the present section (none of which have yet been constructed), the perturbation velocity potential in the space within the wind tunnel is considered analogous to the electrical potential in a dilute electrolyte solution contained in a vessel of the same shape. An insulating material such as Bakelite, the conductivity of which is negligible compared with that of the solution, provides a boundary where the normal potential gradient $\frac{\partial \Phi}{\partial n}$ is zero; and a metal, the conductivity of which is practically infinite relative to that of the solution, serves as a constant-potential boundary along which the longitudinal gradient $\frac{\partial \Phi}{\partial x}$ is zero. In such a setup, current is analogous to velocity except for a difference in sign (in the usual convention, current flows down a voltage gradient

whereas air flows up a velocity-potential gradient); in order to remove this difficulty, the sign convention for electrical potential is reversed in the following discussion.

For greater clarity of exposition, the two-dimensional analogies are treated in detail, the three-dimensional analogies appearing as reasonably obvious extentions or modifications. It will be remembered, however, that any application will be found in three-dimensional problems, inasmuch as most of the two-dimensional problems can be solved analytically.

A two-dimensional vortex may be represented by two long metal plates separated by a thin insulator. (See fig. 6(a).) A flow corresponding to a vortex located at the edge of the plates is set up by applying a difference of potential across the plates. If the perturbation flow that results from the presence of the vortex in the tunnel has a horizontal velocity component, this representation is no longer adequate because it requires the potential to be uniform along each plate. Rigor in this case would require that the plates be composed of a number of separate sections, with each pair separately activated. (See fig. 6(b).) In this way it is possible to provide a potential difference between upper and lower surfaces that is everywhere equal to the desired circulation, without requiring that the potential be uniform along the entire upper surface or lower surface. A horizontal velocity component normally occurs only when the lifting vortex is asymmetrically located in the tunnel. For simplification, only the simpler representation of figure 6(a) is used in the remaining sketches.

The element of lift in three-dimensional flow is the horseshoe vortex of zero span, which is the same as a semi-infinite line of doublets. It may be represented by a pair of long narrow metal strips separated by an insulator. (See fig. 6(c).) As in the two-dimensional analogy, if the lifting element is asymmetrically located in the field the strips must be made up of short pieces, with each pair separately activated. The horseshoe vortex of finite span is represented as in figure 6(d), provided there are no appreciable perturbation velocities in its plane.

Evaluation of interference velocities. The vertical velocity component in the tunnel corresponds to the vertical voltage gradient in the electrolyte, which can be determined by measuring the voltage difference between a pair of short wire electrodes mounted one above the other a fixed distance apart. The tunnel interference at any point is found by measuring this voltage difference (relative to that across the two plates representing the vortex) first in the simulated tunnel and then in a large tank for which the boundary interference is either negligible or so small that it can be adequately computed by simple methods. Since the theoretical flow field for the second case is known, the ratio of these two gradients, together with the distance from the pair of wires to the lifting vortex, should suffice to evaluate the boundary interference. The distance between the pair of wires need not be measured because only the ratio of the gradients is required. Similarly, the exact design and dimensions of the simulated lifting vortex are of no

significance, provided the gradients are determined at reasonable distances from it. In general, boundary interference at the vortex itself cannot be found directly by this method, but may be determined by interpolation between or extrapolation from neighboring points.

Two-dimensional closed-open tunnel. For simplification of the nomenclature, the open tunnel with closed upstream region but without a closed exit is designated the closed-open tunnel. The open tunnel with closed upstream and downstream regions is designated the closed-open-closed tunnel.

Figure 7(a) illustrates the setup for a two-dimensional closed-open tunnel with a vortex on its center line. Shaded lines indicate insulating boundaries, where $\frac{\partial \Phi}{\partial n} = 0$, and heavy unshaded lines indicate metal boundaries on which of is constant. The upstream closed portion should be so long that the potential is essentially uniform at its upstream end: the length indicated on the figure should suffice. The open region should similarly be so long that the vertical flow between the vortex strips and the boundary strips no longer changes with distance downstream; again, the length indicated on the figure should suffice. From the condition of velocity continuity at the entrance lips and the fact that $\frac{\partial \Phi}{\partial x}$ is zero along the free boundaries, it follows that $\frac{\partial \Phi}{\partial x}$ must be zero at the edges of the two closed boundaries. The potentials on the two free boundaries must, therefore, be adjusted until the difference between the potential of each and the potential of a thin feeler electrode just upstream of its edge is zero. For the symmetrical condition shown, the single variable voltage source indicated will provide zero $\frac{\partial \Phi}{\partial x}$ at both edges simultaneously.

Figure 7(b) illustrates the setup for the two-dimensional closedopen tunnel with the vortex in an off-center position. A single variable voltage source across the two free boundaries is now no longer capable of simultaneously satisfying the continuity condition at both edges, so that an additional variable voltage source and an upstream electrode are required. The current in the closed part of the tunnel flowing into this upstream electrode corresponds to an upstream perturbation velocity. This upstream perturbation velocity constitutes the previously mentioned difference between the velocity far upstream in the closed part and the velocity on the free surface. The concept here is slightly at variance with previous discussion, which considered a perturbation velocity along the free surface, with the far upstream velocity appearing as the undisturbed velocity U. As the analogy is set up, however, no perturbation velocity may appear along the free surfaces because they are at constant potential; hence, the total velocity on the free surfaces must be considered as the undisturbed velocity U and any difference between this velocity and the velocity far upstream appears as an upstream perturbation velocity. As appears in part II, this viewpoint is also found convenient in the analytical solution of these problems.

NACA TN No. 1826

Two-dimensional closed-open-closed tunnel .- The setup for the twodimensional closed-open-closed tunnel with a vortex on the center line (fig. 8(a)) is an obvious modification of the corresponding setup for the closed-open tunnel. The same would be true for the off-center vortex except for the necessity of satisfying the condition that the velocities in the upstream and downstream closed regions be equal. Thus, the setup of figure 8(b) provides an upstream perturbation velocity but no downstream perturbation velocity, and cannot, therefore, solve the problem completely. An additional flow, found by the setup of figure 8(c) must be included. An electrode is here located at both the upstream and downstream ends, and the potentials relative to the free boundary are so adjusted that the entrance-lip condition is satisfied. It is apparent that in order to satisfy this condition the downstream current flow will be much greater than the upstream current flow; that is, the downstream perturbation velocity for a contracting or expanding jet is much greater than the upstream perturbation velocity. Because of this difference, a suitable amount of the flow of figure 8(c) may be added to that of figure 8(b) to produce equal upstream and downstream perturbation velocities.

Displacement of the free surfaces. The current density normal to the surface of a metal plate representing a free surface is proportional to $\frac{\partial \Phi}{\partial y}$ and corresponds to the local vertical perturbation velocity. The total vertical displacement at a point on the free surface is then given by $\int \frac{\partial \Phi}{\partial y} dx$ integrated from the entrance lip to the point. In particular, the integral along the entire lower free surface of a closed-

open-closed tunnel represents the displacement at the exit lip and it may be measured by means of an ammeter in the line that goes to the lower metal plate.

If the pressure on the lower free surface can adjust itself so that the displacement at the downstream end is zero, the perturbation velocity at the lower surface will be different from that at the upper surface. If the perturbation velocity on the upper surface is taken as zero, that on the lower surface will be negative, so that the potential on the lower surface must drop uniformly from entrance to exit. Such a variation could be accomplished if the lower surface were represented by a number of short metal strips instead of a single plate.

Three-dimensional closed-open and closed-open-closed tunnels. The analogies for the three-dimensional tunnels are obvious modifications of those for the two-dimensional tunnels. The free boundary may not be simulated by a single metal cylinder because, as was previously noted, different elements of the free boundary do not have the same potential, although the potential is constant along each element. The free boundary must thus be simulated by a number of longitudinal metal strips, insulated from each other, with a feeler electrode immediately in front of each. When the lifting element lies in the horizontal plane of

symmetry, the entrance-lip condition may be satisfied without an additional electrode. If the lifting element is not in the horizontal plane of symmetry, an upstream electrode will be needed, with the potential of each strip adjusted relative to this electrode. For the unsymmetrical closed-open-closed analogy, the requirement that upstream and downstream velocities be equal necessitates further measurements with a setup corresponding to that of figure 8(c).

Acceleration-Potential Analogies

Basic concepts of the analogies. The pressure has the properties of a potential - designated acceleration potential - in a field consisting of a small perturbation flow superposed on a uniform stream. If the pressure in the undisturbed stream is taken as zero, then the perturbation velocities are related to the pressure by the following equations:

$$u = \frac{1}{\rho} \int_{-\infty}^{t} - \frac{\partial p}{\partial x} dt = -\frac{1}{\rho U} \int_{-\infty}^{x} \frac{\partial p}{\partial x} dx = -\frac{p}{\rho U}$$

$$v = \frac{1}{\rho} \int_{-\infty}^{t} - \frac{\partial p}{\partial y} dt = -\frac{1}{\rho U} \int_{-\infty}^{x} \frac{\partial p}{\partial y} dx$$

$$w = \frac{1}{\rho} \int_{-\infty}^{t} - \frac{\partial p}{\partial z} dt = -\frac{1}{\rho U} \int_{-\infty}^{x} \frac{\partial p}{\partial z} dx$$

where

p density

t time

p pressure

Since, by the first equation, u is proportional to p, it is simpler merely to consider the perturbation velocity u itself as the potential, with v and w given by the following equations:

$$A = \int_{-\infty}^{\infty} \frac{\partial \lambda}{\partial n} \, dx$$

and

$$w = \int_{-\infty}^{\infty} \frac{\partial u}{\partial z} dx$$

The necessity of performing an integration in order to determine v or w is a basic disadvantage of the acceleration-potential analogy compared with the velocity-potential analogy in which v and w are measurable directly.

In the analogies to be discussed in the present section, the perturbation velocity u is considered analogous to the electrical potential in a dilute electrolyte solution. A metal serves as a boundary along which u is constant, and the local intensity of current flowing into it gives $\frac{\partial u}{\partial n}$; an insulator serves as a boundary where $\frac{\partial u}{\partial n}$ is zero. The lifting element in either two or three dimensions is represented by a pair of short metal plates separated by an insulator; when the upper plate is maintained at a higher potential than the lower plate, the arrangement represents a thin airfoil with suction (large u) on its upper surface and pressure (small or negative u) on its lower surface. The current at each of the two plates should be the same in order that the slope of the airfoil surface (proportional to v) be the same on both upper and lower sides. In order always to satisfy this condition the voltage source activating the lifting element should not be tapped to any other electrode in the field.

Two-dimensional closed-open tunnel -- The setup for the twodimensional closed-open tunnel with the lifting element on the center line is shown in figure 9(a). The walls of the upstream closed region are represented by insulators, which establish that $\frac{\partial u}{\partial y} = 0$ at every point; hence, the condition that $v = \int_{-\infty}^{\infty} \frac{\partial u}{\partial y} dx = 0$ at every point on the closed boundary is satisfied. The two free boundaries are represented by metal; and electrically connecting them, as shown, satisfies the further condition that they have the same potential (the same u). The flow of current into the lower boundary then equals the flow of current out of the upper boundary, so that the ultimate downstream value of v will be the same on both upper and lower boundaries, as is desired. In fact, for the symmetrical case illustrated, the value of v will be the same at all pairs of opposite points on the two free boundaries; so the boundaries will be everywhere parallel. No special attention need be paid to the entrance lips - the entrance lip condition is automatically satisfied since the potential u is continuous at these points (although the potential gradients at these points are infinite).

For the off-center position of the lifting element (fig. 9(b)) no modification of the circuits is needed. The difference between the potential in the upstream closed region and the potential of the free boundaries, which is the upstream perturbation velocity u, is measured with the aid of the probe P. As in the symmetrical case, the ultimate downstream value of v will be the same for both the upper and the lower boundaries; however, it is no longer true that the two boundaries will be everywhere parallel, and the ultimate width of the jet will be different from the width of the closed part.

Two-dimensional closed-open-closed tunnel. The value of v at the downstream end of the free boundary is given by the total flow of current into the metal plate and, in general, is not zero. At the lip of the closed exit, however, v must be suddenly reduced to zero in order for the flow to follow the solid boundary; hence, a short electrode must be added at the exit lip, and as much current must be forced out of it as flows into the long electrode that represents the open boundary; that is, the integral of $\frac{\partial u}{\partial y}$ dx along the free boundary must be canceled at the exit lip. The setup (fig. 10(a)) therefore shows a voltage source to supply this current and means for measuring and equalizing the current flow into adjacent electrodes. If these additional short electrodes are omitted, the setup will correspond to a tunnel the exit section of which has been alined with the deflected jet (fig. 10(b)) because the condition that $\frac{\partial u}{\partial y} = 0$ on the closed exit boundary would merely permit v to remain at the value it had at the end of the free boundary.

For the off-center position of the lifting surface, a similar setup is used and, as before, probes in the regions far upstream and far downstream are used to determine the potential u in these regions relative to the potential of the free boundary. Since these potentials far upstream and far downstream will not be equal, an additional perturbation field must be provided such that the sum of the two fields will have the same potential in the two regions. This additional perturbation field, which corresponds to a contraction or expansion of the jet, is provided by the setup shown in figure 10(c). It is clear from this figure that the downstream perturbation potential is much greater than the upstream perturbation potential; this result corresponds to that indicated in the velocity-potential analogy.

The condition in which the pressure on the lower free surface is higher than that on the upper free surface is easily represented by applying a voltage difference between the two surfaces. (See fig. 10(d).) The corresponding displacement of the lower surface, however, is not so readily obtained. The vertical velocity at every point is $\int \frac{\partial u}{\partial y} dx$, so that the displacement at each point is $\int \frac{\partial u}{\partial y} dx dx$. In order to accomplish this integration $\frac{\partial u}{\partial y}$ must be determined at points along the boundary, perhaps by breaking the long plate into a number of short pieces and determining the current flowing into each.

Three-dimensional closed-open and closed-open-closed tunnels. The analogies for the three-dimensional tunnels are again obvious modifications of those for the two-dimensional tunnels. For the closed-open analogy, the free boundary may be represented by a single cylinder of metal (fig. ll(a)). For the closed-open-closed analogy, the free boundary must be represented by a number of separate strips (fig. ll(b)) in order that the total current into each strip may be measured and an equal

NACA TN No. 1826

current forced out of the short strip immediately behind it. Contraction or expansion of the jet is represented as in the two-dimensional case; but the setup that would correspond to different pressures along different strips seems to have no practical significance in the three-dimensional case.

Some form of this acceleration-potential analogy is probably the most convenient for solving problems similar to that of the helicopter in the Langley full-scale tunnel. Simply neglecting the exit, as with a closed-open tunnel, permits the free surface to be represented by a single sheet of metal and eliminates any measurements of current flow to or from the surface. Improved accuracy should be attainable by cutting the sheet into two parts with two short strips at the rear. (See fig. ll(c).) The need for many strips seems unlikely, at least in view of the previously mentioned uncertain definition of the physical flow in the region of the exit.

Correspondence between velocity-potential and acceleration-potential analogies.— As has already been indicated, the acceleration potential is identical with the x-component of the perturbation velocity and is hence merely the x-derivative of the perturbation-velocity potential. It is of interest to point out the related fact that the acceleration potential analogies are, in a sense, the x-derivatives of the velocity-potential analogies. For example (see fig. 12),

- (1) For the velocity-potential analogy, an infinitely long double layer represented a lifting element located at its forward edge. The difference between two such double layers, of which one is shifted slightly relative to the other, is merely the short double layer that was used in the acceleration-potential analogy.
- (2) For the velocity-potential analogy, the free boundary consisted of constant-potential strips on which the potentials were so adjusted that the gradient was zero at the leading edge. If each strip is now shifted and subtracted, there remains a long strip, with a short strip at the front and back. Since, in the velocity-potential analogy, the gradient was zero at the entrance lip, the short strip at the front may be neglected. The remainder corresponds to the arrangement used in the acceleration-potential analogy, and the fact that the total current after the subtraction must be zero corresponds to the fact that the total current out of the short strip must be made equal to the total current into the long strip.
- (3) When the lifting element was off-center, the velocity-potential analogies required electrodes upstream and downstream, with uniform current flow along the upstream and downstream closed regions. That the subtraction eliminates these current flows corresponds to the fact that no upstream or downstream electrodes are used in the acceleration-potential analogies.

Technical Difficulties

It should be pointed out that the analogies here described may be rather unwieldy, experimentally. Even for the simplest types of analogies, the literature indicates considerable uncertainty as to the most satisfactory electrolyte and electrode materials, and appreciable difficulty in balancing capacitances (alternating current is generally used in analogies, in order to minimize polarization at the electrodes). In the present analogies, the need for separate current sources that are exactly in phase and the large capacitances that will certainly characterize the vortex and the open-boundary representations should greatly complicate the technique. Perhaps the use of direct current instead of alternating current, with nonpolarizing electrodes (as platinized platinum), would be a more practical approach in this respect. Simultaneously satisfying the entrance-lip condition at a number of points around the inlet (or satisfying the corresponding exit condition for the acceleration-potential analogies) may also turn out to be very difficult.

RÉSUMÉ OF PART I

The most significant points of the preceding discussion of open wind tunnels and their electrical analogies are as follows:

- 1. Continuity of velocity at the lip of the entrance cone is a basic characteristic of the flow in an open wind tunnel.
- 2. Equality of the velocities in the upstream and downstream closed regions is a further condition on the tunnel flow if extraneous longitudinal pressure gradients are to be avoided.
- 3. The velocity on the free surface need not be the same as the velocity in the closed upstream region. In general, the two velocities are the same only when the lifting element lies in the plane of symmetry of the tunnel.
- 4. For the two-dimensional open tunnel the velocities on the two free surfaces need not be equal. If the space below the lower free surface is closed off, the pressure on the lower free surface will adjust itself so that the displacement at the exit lip is zero.
- 5. Considerable uncertainty exists with regard to conditions at the exit or the mathematical equivalents of these conditions. Correspondingly, certain compromises in complying with the idealized downstream conditions may be justified in a determination of boundary interference.
- 6. In any analysis that neglects the closed entrance and exit regions, the condition of zero upstream induced flow must be retained.

7. Electrical analogies of either the velocity-potential or the acceleration-potential type may be devised to correspond to most of the problems discussed.

- 8. In electrical analogies that represent velocity potential by electrical potential, the condition of continuity at the entrance lip appears troublesome, especially for three-dimensional tunnels; however, the exit conditions are easily represented.
- 9. In electrical analogies that represent acceleration potential by electrical potential, the entrance-lip condition is automatically satisfied, but fulfillment of exit conditions is troublesome. Rough approximation of the exit conditions may, however, be adequate for many purposes.
- 10. Acceleration-potential analogies are experimentally simpler than velocity-potential analogies.

II - TWO-DIMENSIONAL TUNNELS

In part II, boundary-induced velocities in two-dimensional open tunnels are derived with special reference to the effects of the closed entrance and exit regions. The cases treated are:

- (1) Tunnel with a closed entrance (upstream) region but without a closed exit region
- (2) Tunnel with a closed entrance region but with only one exit lip (corresponding to a condition in which the downward deflection of the flow is so large that the flow makes contact only with the lower exit lip)
 - (3) Tunnel with closed entrance and exit regions
- (4) Same as case 3, but with different pressures on the two free surfaces

Numerical results are given for all cases.

SYMBOLS AND DIMENSIONS

Each tunnel is idealized as a strip of uniform height h, having a stream velocity V, and containing a point vortex of strength Γ . For simplification of the present development, lengths and velocities will be made nondimensional by dividing by h and V, respectively, and the vortex strength will be made nondimensional by dividing by hV.

Essentially, then, the solutions will be developed for a vortex of strength $\Gamma' = \frac{\Gamma}{hV}$ in a tunnel of unit height; and in the following list of symbols the lengths in the complex planes are in terms of h, and the complex velocities are in terms of V:

h	tunnel height
V	tunnel velocity
ζ	complex variable of physical plane ($\xi + i\eta$)
^{\$} 1	location of vortex in &-plane
Z	complex variable of transformed plane (x + iy)
zl	location of vortex in z-plane
g	complex velocity in physical plane (u - iv)
Q	complex velocity in transformed plane (u - iv)
A, B, C, M, N	real constants
Г	vortex strength
L.e	nondimensional vortex strength $\left(\frac{\Gamma}{hV}\right)$
q ₁ (ζ,ζ ₁)	induced complex velocity at ζ when vortex is at ζ 1.
$q_1(\zeta_1)$	induced complex velocity at 51
a	abscissa of exit lip in transformed space
wl	a complex velocity in the form of an elliptic integral of the first kind
w2	a complex velocity in the form of an elliptic integral of the second kind
w ₃	a complex velocity
7	variable of integration
G	function defined by equation (2)

K, K'	complete elliptic integrals of the first kind, with modulus 1/a
Е, Е'	when not followed by parenthesis, complete elliptic integrals of the second kind, with modulus 1/a; with upper limit indicated in parentheses, incomplete elliptic integrals of the second kind, with modulus 1/a
F, F'	incomplete elliptic integrals of the first kind, with modulus 1/a, and with upper limit indicated in parentheses
R.P.	real part
I.P.	imaginary part
c	airfoil chord
cl	airfoil lift coefficient
€	tunnel-induced angle, radians
u _b	horizontal perturbation velocity at free boundary
Subscript	
i	induced

BOUNDARY CONDITIONS

The two-dimensional tunnels discussed are considered to have their fixed and free boundaries parallel to the real axis, with the main tunnel flow from left to right. The physical plane (in which lengths and velocities have been made nondimensional as just described) will be designated the ζ -plane, with the complex perturbation velocity u - iv, or $q(\zeta)$, subject to the following conditions:

- (1) on each fixed (or closed) boundary, I.P.q(ζ) = -v = 0
- (2) On each free (or open) boundary, $R \cdot P \cdot q(\zeta) \equiv u = 0$ or a constant
- (3) At each lip of the closed entrance section, $q(\zeta)$ is continuous

CASE 1 - CLOSED-OPEN TUNNEL

Total perturbation velocity. - By the transformation

$$z = e^{\pi \zeta} \tag{1}$$

the tunnel in the ζ -plane, represented by an infinitely long strip of unit height, is transformed to the upper half of the z-plane. The correspondence between points is shown in figure 13.

The complex velocity (rather than the more usual complex potential) is considered to be retained in the transformation, and the problem is thus to find a function Q(z), where

$$u - iv = Q(z) = g(\zeta)$$

such that

(1) On the closed sections of the boundary, that is, for z real and |z| < 1,

$$I \cdot P \cdot Q(z) = 0$$

(2) On the open sections of the boundary, that is, for z real and |z| > 1,

$$R \cdot P \cdot Q(z) = 0$$

(3) For $z = \pm 1$,

$$Q(z) = 0$$

(4) Q(z) is finite at infinity

Consider the complex velocity G(z) corresponding to a vortex at z_1 and its reflection at z_1 :

$$G(z) = i\left(\frac{1}{z - z_1} - \frac{1}{z - \overline{z_1}}\right) \tag{2}$$

This function, which is of order $1/z^2$ at infinity, satisfies conditions (1) and (4) but not (2) and (3). Functions of the form $\sqrt{1-z^2}$, $z\sqrt{1-z^2}$, . . . satisfy conditions (1), (2), and (3). At infinity, $\sqrt{1-z^2}$ is of order z and $z\sqrt{1-z^2}$ is of order z^2 ; therefore,

either of the products $G\sqrt{1-z^2}$, $Gz\sqrt{1-z^2}$, or a linear combination of the two satisfies the four conditions and has a pole of the first order at z_1 . These facts suggest that the desired velocity function is of the form

$$Q(z) = i\left(\frac{1}{z - z_1} - \frac{1}{z - \bar{z}_1}\right)(A + Bz)\sqrt{1 - z^2}$$
 (3)

21

where A and B are as yet undetermined real constants.

The values of A and B are to be determined such that the pole at z_1 represents a vortex of strength Γ' in the ζ -plane. Thus

$$\Gamma' = \oint g(\zeta) d\zeta = \oint Q(z) \frac{d\zeta}{dz} dz = \frac{1}{\pi} \oint Q(z) \frac{dz}{z}$$

where the integral is taken about the point z₁. By Cauchy's integral formula

$$\Gamma' = -2(A + Bz_1) \frac{\sqrt{1 - z_1^2}}{z_1}$$
 (4)

The values of Γ^1 and z_1 are known, so that this complex equation can be solved for the two real constants A and B. Substituting these values in equation (3) will thus give the desired complex velocity function.

Tunnel-interference velocity - The tunnel-interference velocity is defined as the difference between the total perturbation velocity $q(\zeta)$ due to the presence of the vortex in the tunnel and the velocity due to a vortex in an unbounded medium. That is, the tunnel-interference velocity $q_1(\zeta,\zeta_1)$ is

$$q_{1}(\zeta,\zeta_{1}) = i\left(\frac{1}{z-z_{1}} - \frac{1}{z-\overline{z}_{1}}\right) (A + Bz) \sqrt{1-z^{2}} + \frac{i\Gamma'}{2\pi(\zeta-\zeta_{1})}$$
 (5)

If the vortex is on the axis of the tunnel, that is, if $\zeta_1 = \xi_1 + \frac{1}{2}$, then from equation (1), $z_1 = iy_1$, and equation (4) gives

$$B = -\frac{\Gamma'}{2\sqrt{1 + y_1^2}}$$
(6)

If the point of evaluation is also on the axis (that is, $\zeta = \xi + \frac{1}{2}$, whence z = iy), then

$$q_{\frac{1}{2}}\left(\xi + \frac{1}{2}, \xi_{1} + \frac{1}{2}\right) = -i\Gamma' \frac{yy_{1}}{y^{2} - y_{1}^{2}} \sqrt{\frac{y^{2} + 1}{y_{1}^{2} + 1}} + \frac{i\Gamma'}{2\pi(\xi - \xi_{1})}$$
(7)

Thus, if the vortex is on the axis, the interference velocity at all points on the axis has only a vertical component.

The interference velocity at the vortex itself is the limit of expression (5) as z approaches z_1 . The term containing $z - \bar{z}_1$ offers no difficulties and its limit is readily evaluated:

$$\lim_{z \to z_1} - \frac{i}{z - \bar{z}_1} (A + Bz) \sqrt{1 - z^2} = -\frac{1}{2y_1} (A + Bz_1) \sqrt{1 - z^2} = \frac{\Gamma^1 z_1}{4y_1}$$

where the last equality follows from equation (4). The remainder of equation (5), after $\pi(\zeta - \zeta_1)$ is replaced by $\log \frac{z}{z_1}$, is

$$i \left[\frac{(A + Bz)\sqrt{1 - z^2}}{z - z_1} + \frac{\Gamma'}{2 \log \frac{z}{z_1}} \right] = i \frac{(A + Bz)\sqrt{1 - z^2} \log \frac{z}{z_1} + \frac{\Gamma'}{2}(z - z_1)}{(z - z_1)\log \frac{z}{z_1}}$$

This expression is of the form $\frac{0}{0}$ for $z=z_1$. Differentiating numerator and denominator, according to L'Hôspital's rule still leaves both equal to zero at $z=z_1$ (that the derivative of the denominator is zero at $z=z_1$ is obvious; that the derivative of the numerator is also zero at $z=z_1$ can be verified with the aid of equation (4)). A second differentiation yields the following expression for the limit as z approaches z_1 :

$$-(A + Bz_1)\sqrt{1 - z_1^2} - \frac{2(A + Bz_1)z_1^2}{\sqrt{1 - z_1^2}} + 2Bz_1\sqrt{1 - z_1^2}$$

$$= \frac{2z_1}{2z_1}$$

This fraction can be greatly simplified by use of equation (4), and the result, added to the previously derived limit, gives the desired correction at the vortex:

$$\lim_{\xi \to \xi_1} q_i(\xi, \xi_1) = q_i(\xi_1) = i \left[-\frac{\Gamma!}{4} + \frac{\Gamma!}{2(1 - z_1^2)} + B\sqrt{1 - z_1^2} + \frac{\Gamma'z_1}{4iy_1} \right]$$
(8)

For the special case in which the vortex is on the tunnel axis (z = iy), this expression reduces to the following form (after substituting for B from equation (6)):

$$q_{1}(\xi + \frac{1}{2}) = -\frac{1\Gamma'}{2} \frac{y_{1}^{2}}{1 + y_{1}^{2}}$$
 (9)

Upstream perturbation velocity - If the vortex is not on the tunnel axis, A will not be zero (compare equation (6)). The tunnel interference velocity far upstream in the closed part of the tunnel is found by putting $\zeta = -\infty$ and z = 0 in equation (5), which then reduces to

$$q_1(-\infty, \zeta_1) = iA\left(\frac{1}{\tilde{z}_1} - \frac{1}{z_1}\right) = -\frac{2Ay_1}{|z_1|^2}$$

which is real. For this unsymmetrical case, therefore, a finite longitudinal perturbation velocity is found far upstream in the closed part. As was pointed out in part I, such results appear because the problem was set up so that the longitudinal perturbation velocity on the open boundary is zero. If the velocity far upstream in the closed part is to be taken as the base, the result means merely that the longitudinal velocity on the open boundary exceeds this base velocity by $\frac{2Ay_1}{|z_1|^2}$ and that there is a corresponding difference in pressure between the closed part and the space surrounding the jet.

Limiting case of completely open tunnel. With increasing distance of the vortex from the closed entrance (that is, with increasing y_1), expression (9) approaches $-\frac{i\Gamma^1}{2}$. As was pointed out in part I, the

image system normally used to satisfy the boundary condition on an infinitely long, open, two-dimensional tunnel produces no induced flow at the vortex itself, and only after introduction of the additional condition that the upstream flow be horizontal is this value of $-\frac{i\Gamma'}{2}$

for the induced-flow correction obtained. In the present development, however, it is seen that the condition of continuity at the entrance lips automatically takes care of this condition on the upstream flow direction, even when the entrance and the vortex are infinitely far apart.

No further discussion of the completely open tunnel will be given here inasmuch as this case has been adequately treated by the method of images. (See reference 6, p. 302.)

CASE 2 - TUNNEL WITH ONE FIXED EXIT BOUNDARY

Perturbation velocity. As before, the transformation $z=e^{\pi \zeta}$ transforms the tunnel, considered as an infinite strip of unit height, into the upper half of the z-plane. The correspondence between points is shown in figure 14. The conditions on the complex velocity Q(z) are:

- (1) On the real axis, $I \cdot P \cdot Q(z) = 0$ for -1 < z < 1 and for z > a
- (2) On the real axis, $R \cdot P \cdot Q(z) = 0$ for z < -1 and for 1 < z < a
- (3) For $z = \pm 1$, Q(z) = 0
- (4) Q(z) is finite everywhere in the upper half-plane except at z=a and at $z=z_1$. As noted in part I, Q(z) will be infinite at z=a

The function G(z), given by equation (2), will again be used as a factor that is real along the entire real axis and has the desired type of singularity at z₁. The functions $\sqrt{\frac{1-z^2}{a-z}}$ and $z\sqrt{\frac{1-z^2}{a-z}}$ change from pure real to pure imaginary as z passes through ±1 or through a, and, furthermore, are zero at z = ±1 and infinite at z = a. At infinity they are of order $z^{1/2}$ and $z^{3/2}$, respectively. Therefore, as before, a linear combination of $G(z)\sqrt{\frac{1-z^2}{a-z}}$ and $G(z)z\sqrt{\frac{1-z^2}{a-z}}$

satisfies the preceding conditions and has a pole of the first order at z_1 . Q(z) is therefore of the form:

$$Q(z) = i \left(\frac{1}{z - z_1} - \frac{1}{z - \overline{z}_1} \right) (A + Bz) \sqrt{\frac{1 - z^2}{a - z}}$$
 (10)

The real constants A and B are determined by the same condition as before, which gives

$$\Gamma' = -\frac{2(A + Bz_1)}{z_1} \sqrt{\frac{1 - z_1^2}{a - z_1}}$$
 (11)

Tunnel-interference velocity - The interference velocity $q_1(\zeta, \zeta_1)$ is the difference between the perturbation velocity and the velocity due to a vortex located at the same point in an unbounded medium:

$$q_{1}(\zeta, \zeta_{1}) = i\left(\frac{1}{z-z_{1}} - \frac{1}{z-\overline{z}_{1}}\right)(A + Bz)\sqrt{\frac{1-z^{2}}{a-z}} + \frac{i\Gamma'}{2\pi(\zeta-\zeta_{1})}$$
 (12)

This expression does not simplify appreciably if the vortex is located on the axis, and the interference velocity at a point on the axis due to a vortex on the axis is not normal to the axis.

The interference velocity at the vortex itself is the limit of expression (12) as z approaches z₁. Proceeding as in the preceding case gives:

$$q_{i}(\zeta_{1}) = i \frac{\Gamma'}{2(1-z_{1}^{2})} - \frac{\Gamma'a}{4(a-z_{1})} + B\sqrt{\frac{1-z_{1}^{2}}{a-z_{1}}} + \frac{\Gamma'z_{1}}{4iy_{1}}$$
(13)

It may be shown with the aid of equation (11) that this equation reduces to that for the closed-open tunnel as a goes to infinity.

CASE 3 - CLOSED-OPEN-CLOSED TUNNEL

Perturbation velocity. The transformation $z=e^{\pi\zeta}$ transforms the tunnel space into the upper half of the z-plane with correspondence between points as indicated in figure 15. The boundary conditions on the complex velocity Q(z) are:

- (1) On the real axis, I.P.Q(z) = 0 for |z| < 1 and for |z| > a
- (2) On the real axis, $R \cdot P \cdot Q(z) = 0$ for 1 < |z| < a
- (3) For $z = \pm 1$, Q(z) = 0
- (4) Q(z) is finite everywhere in the upper half-plane except at $z=\pm a$ and at $z=z_1$
- (5) $Q(0) = Q(\infty)$, (this equation corresponding to the condition noted in part I that the perturbation velocities in the upstream and downstream closed regions be the same)

The function G(z) given by equation (2) is again used as a factor of Q(z). The functions $\sqrt{\frac{1-z^2}{a^2-z^2}}$, $z\sqrt{\frac{1-z^2}{a^2-z^2}}$, and $z^2\sqrt{\frac{1-z^2}{a^2-z^2}}$ satisfy

conditions (1), (2), and (3), and are of orders 1, z, and z^2 at infinity, respectively. By the same reasoning as before,

$$Q(z) = i\left(\frac{1}{z - z_1} - \frac{1}{z - \overline{z}_1}\right)(A + Bz + Cz^2)\sqrt{\frac{1 - z^2}{a^2 - z^2}}$$
 (14)

The condition that the pole of the first order at z_1 represents a vortex of strength Γ' is:

$$\Gamma' = -\frac{2(A + Bz_1 + Cz_1^2)}{z_1} \sqrt{\frac{1 - z_1^2}{a^2 - z_1^2}}$$
 (15)

Condition (5) is satisfied by equating the two forms of equation (14) for z equal to zero and equal to infinity. Thus

$$Q(0) = i\left(-\frac{1}{z_1} + \frac{1}{\overline{z}_1}\right) \frac{A}{a}$$

$$= \frac{-2y_1}{|z_1|^2} \frac{A}{a}$$

$$\lim_{Z \to \infty} Q(z) = \lim_{Z \to \infty} \frac{-2y_1}{(z - z_1)(z - \overline{z}_1)} (A + Bz + Cz^2) \sqrt{\frac{1 - z^2}{a^2 - z^2}}$$

$$= -2y_1C$$

whence, by condition (5)

$$\frac{-2y_1}{|z_1|^2} \frac{A}{a} = -2y_1C$$

or

$$C = \frac{A}{a|z_1|^2} \tag{16}$$

The complex equation (15) and the real equation (16) suffice for evaluating the three real constants A, B, and C in equation (14).

Tunnel-interference velocity .- The tunnel interference velocity is

$$q_{i}(\zeta,\zeta_{1}) = i\left(\frac{1}{z-z_{1}} - \frac{1}{z-\overline{z}_{1}}\right)(A + Bz + Cz^{2})\sqrt{\frac{1-z^{2}}{a^{2}-z^{2}}} + \frac{i\Gamma'}{2\pi(\zeta-\zeta_{1})}$$
 (17)

If the vortex is on the tunnel axis, that is, if $z_1 = iy_1$, equation (15) gives

$$B = -\frac{\Gamma'}{2} \sqrt{\frac{a^2 + y_1^2}{1 + y_1^2}}$$

$$C = \frac{A}{y_1^2}$$
(18)

Comparing this last equation with equation (16), which reduces to the following form for $z_1 = iy_1$

$$C = \frac{A}{ay_1^2}$$

shows that for this symmetrical case

$$A = C = 0$$

or

since, as is clear from figure 15, a \neq 1. The interference velocity at a point on the axis (z = iy) due to a vortex on the axis is thus

$$q_{1}\left(\xi+\frac{1}{2},\xi_{1}+\frac{1}{2}\right) = -\frac{i\Gamma'y_{1}y}{y^{2}-y_{1}^{2}}\sqrt{\frac{1+y^{2}}{a^{2}+y^{2}}}\frac{a^{2}+y_{1}^{2}}{1+y_{1}^{2}} + \frac{i\Gamma'}{2\pi(\xi-\xi_{1})}$$
(19)

which is normal to the axis.

The interference velocity at the vortex itself is the limit of expression (17) as z approaches z₁. Proceeding as before gives

$$q_{i}(\zeta_{1}) = i \frac{\Gamma'}{4} + \frac{\Gamma'z_{1}^{2}}{2} \frac{a^{2} - 1}{\left(a^{2} - z_{1}^{2}\right)\left(1 - z_{1}^{2}\right)} + \left(B + 2Cz_{1}\right)\sqrt{\frac{1 - z_{1}^{2}}{a^{2} - z_{1}^{2}}} + \frac{\Gamma'z_{1}}{4iy_{1}}$$
(20)

For the case in which the vortex is on the axis $(z_1 = iy_1)$ the normal velocity at the free boundary (z = x, where 1 < x < a) is given by

$$Q(x) = i\left(\frac{1}{x - iy_1} - \frac{1}{x + iy_1}\right)Bx\sqrt{\frac{1 - x^2}{a^2 - x^2}}$$

$$Q(x) = \frac{2iy_1}{x^2 + y_1^2}Bx\sqrt{\frac{x^2 - 1}{a^2 - x^2}}$$
(21)

CASE 4 - CLOSED-OPEN-CLOSED TUNNEL WITH UNEQUAL

PRESSURES ON THE FREE SURFACES

Boundary conditions -- As indicated in part I, the two-dimensional closed-open-closed tunnel may develop unequal pressures on the two free surfaces if a closed space exists below the lower free surface. Within the limits of the present linear theory, this pressure difference corresponds to superposing on the flow discussed in the preceding section an additional perturbation velocity field Q(z) that

- (1) Has no singularities within the tunnel
- (2) Satisfies the condition of continuity at the inlet lips

- (3) Has a horizontal component equal to, say, +1 on the upper free boundary and -1 on the lower free boundary
 - (4) Has no vertical component on the closed boundaries
 - (5) Is zero at infinity upstream and downstream

Rewritten as conditions on the complex velocity Q(z) in the z-plane (fig. 15), these conditions become

- (1) Q(z) has no singularities in the upper half of the z-plane
- (2) Q(z) = 0 at $z = \pm 1$
- (3) On the real axis, Q(z) = -1 for 1 < z < a, and Q(z) = +1 for -a < z < -1
 - (4) On the real axis, I.P.Q(z) = 0 for |z| < 1 and for |z| > a
 - (5) Q(z) = 0 for z = 0 and for $z = \infty$

Outline of method. - Consider the following two functions of z:

$$w_1 = \int_0^z \frac{dz}{\sqrt{(1 - z^2)(a^2 - z^2)}}$$

$$w_2 = \int_0^z \sqrt{\frac{a^2 - z^2}{1 - z^2}} dz$$

They can be considered as complex velocities having the following properties along the real axis (compare reference 10):

 w_1 is real between 1 and -1; between 1 and a, or between -1 and -a, its real part is constant but an imaginary part is introduced; beyond a or -a, the imaginary part is constant while the real part approaches zero; $R \cdot P \cdot w_1(z) = -R \cdot P \cdot w_1(-z)$; $I \cdot P \cdot w_1(z) = I \cdot P \cdot w_1(-z)$

 w_2 has the same properties as w_1 except that beyond a and -a its real part approaches ∞ and $-\infty$, respectively

Maps of the two functions are shown in figure 16. It should obviously be possible to find a linear combination of these two functions, Mw_1 + Nw_2 , such that for 1 < z < a

$$R \cdot P \cdot \left(Mw_1 + Nw_2\right) = -1$$

for -a < z < -1

$$R \cdot P \cdot (Mw_1 + Nw_2) = +1$$

and beyond a or -a

$$I \cdot P \cdot \left(Mw_1 + Nw_2\right) = 0$$

A simple additional function w₃ to be discussed subsequently is needed to satisfy the condition at infinity. The desired velocity function for the closed-open-closed tunnel with unequal pressures is thus of the form:

$$Q(z) = Mw_1(z) + Nw_2(z) + w_3(z)$$

The constants M and N are derived in the two following sections.

Evaluation of integrals. In the following development, the modulus of all the elliptic integrals is 1/a; the modulus will therefore not be indicated in the symbols. In the designations for the incomplete elliptic integrals, E, E', F, and F', the terms in parentheses are the upper limits of integration. Then

$$w_{1}(1) = R \cdot P \cdot w_{1}(a) = \int_{0}^{1} \frac{dz}{\sqrt{(1 - z^{2})(a^{2} - z^{2})}} = \frac{1}{a}K$$

$$w_{2}(1) = R \cdot P \cdot w_{2}(a) = \int_{0}^{1} \sqrt{\frac{a^{2} - z^{2}}{1 - z^{2}}} dz = aE$$

I.P.w₁(a) =
$$\int_{1}^{a} \frac{dz}{\sqrt{(1-z^2)(a^2-z^2)}}$$

which by the substitution $z^2 = a^2 - (a^2 - 1)l^2$ reduces to

$$\frac{i}{a} \int_{0}^{1} \frac{dl}{\sqrt{(1-l^{2})(1-\frac{a^{2}-1}{a^{2}}l^{2})}} = \frac{i}{a}K'$$

I.P.w₂(a) =
$$\int_{1}^{a} \sqrt{\frac{a^2 - z^2}{1 - z^2}} dz$$

which by the substitution $z^2 = a^2 - (a^2 - 1)i^2$ reduces to

$$= ia \int_{0}^{1} \frac{dl}{\sqrt{(1-l^{2})(1-\frac{a^{2}-1}{a^{2}}l^{2})}} - ia \int_{0}^{1} \sqrt{\frac{1-\frac{a^{2}-1}{a^{2}}l^{2}}{1-l^{2}}} dl$$

= iaK' - iaE'

Solution of simultaneous equations for M and N.- With the aid of the four formulas just derived, the two previously mentioned equations in M and N may be written

$$\frac{M}{8}K + NaE = -1$$

$$\frac{M}{a}K' + NaK' - NaE' = 0$$

which are easily solved simultaneously for M and N. By introducing the following relation between the complete elliptic integrals (reference 11, p. 520)

$$EK' - KK' + KE' = \frac{\pi}{2}$$

the expressions for M and N are finally obtained in the following forms:

$$M = \frac{2a}{\pi} (K' - E')$$

$$N = -\frac{2K^{\dagger}}{a\pi}$$

Value of $Mw_1 + Nw_2$ at infinity. The constants M and N have been determined so that I.P. $(Mw_1 + Nw_2) = 0$ at infinity; furthermore, R.P.Mw₁ = 0 at infinity, as is clear from figure 16. Therefore, the value of $Mw_1 + Nw_2$ at infinity is merely R.P.Nw₂ at infinity. It is necessary to investigate this limit before choosing the form of w_3 , because, as was previously noted, the purpose of w_3 is to provide Q(z) = 0 at infinity. The limit may be written

$$\text{R.P.Nw}_{2}(\infty) = \text{N} \int_{0}^{1} \sqrt{\frac{a^{2} - z^{2}}{1 - z^{2}}} dz + \text{N} \int_{a}^{\infty} \sqrt{\frac{a^{2} - z^{2}}{1 - z^{2}}} dz$$

The first term is simply NaE. In order to evaluate the second term, substitute $z = \frac{a}{l}$

$$N \int_{a}^{\infty} \sqrt{\frac{a^2 - z^2}{1 - z^2}} dz$$

$$= Na^{2} \int_{0}^{1} \sqrt{\frac{1 - i^{2}}{a^{2} - i^{2}}} \frac{di}{i^{2}}$$

$$= Na^{2} \int_{0}^{1} \frac{(1 - i^{2})}{\sqrt{(1 - i^{2})(a^{2} - i^{2})}} \frac{di}{i^{2}}$$

$$= - Na^{2} \int_{0}^{1} \frac{di}{\sqrt{(1 - i^{2})(a^{2} - i^{2})}} + Na^{2} \int_{0}^{1} \frac{di}{i^{2} \sqrt{(1 - i^{2})(a^{2} - i^{2})}}$$

The first term is -NaK. In order to evaluate the second term, it is noted (reference 12) that

$$\frac{d}{dl} \sqrt{\frac{(1-l^2)(a^2-l^2)}{l}}$$

$$= \frac{l^4-a^2}{l^2\sqrt{(1-l^2)(a^2-l^2)}}$$

$$= \frac{-a^2}{l^2\sqrt{(1-l^2)(a^2-l^2)}} + \frac{l^2-a^2}{\sqrt{(1-l^2)(a^2-l^2)}} + \frac{a^2}{\sqrt{(1-l^2)(a^2-l^2)}}$$

Transposing terms in this equation gives

$$\frac{a^{2}}{i^{2}\sqrt{(1-i^{2})(a^{2}-i^{2})}} = \frac{a^{2}}{\sqrt{(1-i^{2})(a^{2}-i^{2})}} - \sqrt{\frac{a^{2}-i^{2}}{1-i^{2}}}$$
$$-\frac{d}{di}\frac{\sqrt{(1-i^{2})(a^{2}-i^{2})}}{i}$$

whence

$$Na^{2} \int_{0}^{1} \frac{dt}{t^{2} \sqrt{(1 - t^{2})(a^{2} - t^{2})}} = Na^{2} \int_{0}^{1} \frac{dt}{\sqrt{(1 - t^{2})(a^{2} - t^{2})}}$$

$$-N \int_{0}^{1} \sqrt{\frac{a^{2} - t^{2}}{1 - t^{2}}} dt$$

$$-N \frac{\sqrt{(1 - t^{2})(a^{2} - t^{2})}}{t} \Big|_{0}^{1}$$

$$= NaK - NaE - N \frac{\sqrt{(1 - t^{2})(a^{2} - t^{2})}}{t} \Big|_{0}^{1}$$

The first two terms on the right are exactly canceled by the two terms previously obtained, so that the final result is:

$$\lim_{z \to \infty} R \cdot P \cdot Nw_2(z) = \lim_{l \to 0} -N \frac{\sqrt{1 - l^2/(a^2 - l^2)}}{l} \Big|_0^1$$

$$= \lim_{z \to \infty} Nz \sqrt{1 - \frac{a^2}{z^2}} \sqrt{1 - \frac{1}{z^2}}$$

$$= \lim_{z \to \infty} Nz - \frac{N}{z} \left(\frac{a^2 + 1}{2}\right) - \cdots$$

Derivation of w_3 . In order to cancel the effect of the terms $Mw_1 + Nw_2$ at infinity, the function w_3 must approach $-R.P.Nw_2(z)$ as z increases without limit. In addition, it must have no singularities in the upper half of the z-plane, it must satisfy the condition of continuity at $z = \pm 1$, it must be a pure real on the fixed boundaries and a pure imaginary on the free boundaries, and it must be zero at z = 0. It is readily formulated as

$$w_3(z) = -Nz \sqrt{\frac{1 - z^2}{a^2 - z^2}}$$

That this function satisfies the first condition is readily shown by writing it in a slightly different form and expanding the radical:

$$\lim_{z \to \infty} -Nz \sqrt{\frac{1-z^2}{a^2-z^2}} = \lim_{z \to \infty} -Nz \sqrt{\frac{1-\frac{1}{z^2}}{1-\frac{a^2}{z^2}}}$$

$$= \lim_{z \to \infty} -Nz \left(1 + \frac{a^2-1}{2z^2} + \dots\right)$$

$$= \lim_{z \to \infty} -Nz - \frac{N(a^2-1)}{2z} - \dots$$

Comparison of this expression with that for $\lim_{z\to\infty} R \cdot P \cdot Nw_2(z)$ shows that

the difference between the two expressions approaches zero as z approaches infinity. That the function satisfies the remaining conditions is readily verified by inspection.

The complex velocity function for the closed-open-closed tunnel with unequal pressures is, finally,

$$Q(z) = \frac{2a}{\pi} (K' - E') \int_{0}^{z} \frac{dz}{\sqrt{1 - z^{2}} (a^{2} - z^{2})}$$

$$- \frac{2K'}{a\pi} \int_{0}^{z} \sqrt{\frac{a^{2} - z^{2}}{1 - z^{2}}} dz + \frac{2K'}{a\pi} z \sqrt{\frac{1 - z^{2}}{a^{2} - z^{2}}}$$
(22)

or

$$Q(z) = \frac{2}{\pi} (K' - E') F(z) - \frac{2K'}{\pi} E(z) + \frac{2K'}{a^2 \pi} z \sqrt{\frac{1 - z^2}{1 - \frac{z^2}{a^2}}}$$
(23)

where the modulus of the elliptic integrals is 1/a.

Induced velocity on the axis. For the special case in which z=iy, the preceding equations for Q reduce to a somewhat simpler form. The procedure will be only outlined here, inasmuch as the manipulative steps are similar to those already described.

Replacing z with iy in the expression for w₁ and then substituting $y^2 = \frac{a^2}{l^2} - a^2$ reduces the first term to

$$\frac{2i}{\pi}(K' - E')\left[K' - F'\left(\frac{1}{\sqrt{1 + \frac{y^2}{a^2}}}\right)\right]$$

The same substitutions, together with the previously described technique from reference 12 reduces the second term to

$$-\frac{2iK'}{\pi} \left\{ \frac{y}{a^2} \sqrt{\frac{1+y^2}{1+\frac{y^2}{a^2}}} + \left[K' - F' \left(\frac{1}{1+\frac{y^2}{a^2}} \right) - \left[E' - E' \left(\frac{1}{1+\frac{y^2}{a^2}} \right) \right] \right\}$$

The third term is found directly as

$$\frac{2iK!}{a^2\pi}y\sqrt{\frac{1+y^2}{1+\frac{y^2}{a^2}}}$$

The total simplifies to the form

$$Q(iy) = \frac{2i}{\pi} \left[-K'E' \left(\frac{1}{\sqrt{1 + \frac{y^2}{8^2}}} \right) + E'F' \left(\frac{1}{\sqrt{1 + \frac{y^2}{8^2}}} \right) \right]$$
 (24)

Normal velocity and normal displacement at the free surface. The normal velocity on the free surface may be written in the following form:

I.P.Q(x) =
$$\frac{2i}{\pi}$$
(K' - E') $\int_{1}^{x} \frac{dx}{\sqrt{(x^2 - 1)(1 - \frac{x^2}{a^2})}}$

$$- \frac{2iK'}{\pi} \int_{1}^{x} \sqrt{\frac{1 - \frac{x^2}{a^2}}{x^2 - 1}} dx - \frac{2iK'}{a^2\pi} x \sqrt{\frac{x^2 - 1}{1 - \frac{x^2}{a^2}}}$$

By the substitution of $x^2 = a^2 - (a^2 - 1)l^2$, the integrals are readily reduced to standard forms of incomplete elliptic integrals, and the equation takes the form

$$I \cdot P \cdot Q(x) = \frac{2i}{\pi} \left[E' F' \left(\frac{a^2 - x^2}{a^2 - 1} \right) - K' E' \left(\frac{a^2 - x^2}{a^2 - 1} \right) \right] - \frac{2iK'}{a^2 \pi} x \sqrt{\frac{x^2 - 1}{1 - \frac{x^2}{a^2}}}$$
(25)

The normal displacement, or distortion, of the free surface is found by integrating this expression along the free surface in the physical plane:

Normal displacement at
$$x = \int_{1}^{x} I \cdot P \cdot Q(x) d\xi$$

$$= \int_{1}^{x} I \cdot P \cdot Q(x) \frac{dx}{\pi x}$$

The integral may be evaluated numerically; however, the third term of $I \cdot P \cdot Q(x)$ is amenable to analytical treatment:

$$-\frac{2iK!}{a^{2}\pi} \int_{1}^{x} x \sqrt{\frac{x^{2}-1}{1-\frac{x^{2}}{a^{2}}}} \frac{dx}{\pi x} = -\frac{2iK!}{a^{2}\pi^{2}} \int_{1}^{x} \sqrt{\frac{x^{2}-1}{1-\frac{x^{2}}{a^{2}}}} dx$$

$$= -\frac{2iK!}{\pi^{2}} \left\{ \left[E' - E' \left(\frac{a^{2}-x^{2}}{a^{2}-1} \right) \right] - \frac{1}{a^{2}} \left[K' - F' \left(\frac{a^{2}-x^{2}}{a^{2}-1} \right) \right] \right\}$$

At the edge of the exit lip, where x = a, this expression reduces to

$$-\frac{2iK'}{\pi^2}\left(E'-\frac{K'}{a^2}\right)$$

NUMERICAL RESULTS

In the following sections are described some numerical results that were computed by the preceding equations in order to show the magnitudes of the entrance and exit effects. It will be noted that, since the complex velocity has been made nondimensional by dividing by V, the component v is identical with the tunnel-induced angle ϵ , in radians, and the component u is the fractional increase in the horizontal velocity. The equivalence of the two ordinate scales indicated in the plots of the results follows from the equation

$$\frac{\Gamma}{\Lambda} = \frac{cc^{3}}{2}$$

Closed-open tunnel .- In figure 17 are shown calculated values of the induced downwash angle along the tunnel axis for various positions of the lifting vortex along the axis. The figure shows that for $\xi_1 = 1.0$ and 1.5, the induced angles at the vortex itself ($\xi = 1.0$ and 1.5, respectively) are almost exactly $\frac{\Gamma'}{2}$, which is the value for an infinitely long open tunnel; and, furthermore, the two curves are symmetrical about the point $\xi = \xi_1$. In fact, within the accuracy of the plot, these two curves are identical with the curve for an infinitely long open tunnel. It may be concluded that the closed entrance has no effect if the vortex is more than one tunnel height from the entrance. For $\xi_1 = 0.5$, which is a more likely location of the wing, the induced velocity at $\xi = \xi_1$, is 0.481', and the curve is no longer exactly symmetrical about the point $\xi = \xi_1$; however, these differences from the conditions for the infinitely long open tunnel are too small to be practically significant, so that the usual infinite-open-tunnel theory is still adequate for $\xi_1 = 0.5$. For ξ_1 less than 0.5, the deviations from infiniteopen-tunnel theory become larger rapidly, until, when the vortex is in the plane of the entrance $(\xi_1 = 0)$, the induced angle at the point $\xi = \xi_1$ is only $\frac{1}{4}$.

A similar discussion applies for the vortex in the closed portion of the tunnel $(\xi_1 < 0)$, although this case normally has no practical significance. For $\xi_1 = -1$, the induced angles in the neighborhood of the vortex are practically identical with those for an infinitely long closed tunnel; however, in the open region $(\xi > 0)$, the curve is considerably different from that for the infinitely long closed tunnel (shown as the dashed curve in fig. 17).

Symmetrical closed-open-closed tunnel. In figure 18 are shown similar curves for a symmetrical closed-open-closed tunnel of which the length of the open section is 1.5 times the tunnel height. All curves show a sharp reduction in the induced angle as the closed exit is approached and entered; however, for $\xi_1 < 1$, the closed exit has practically no effect on the induced velocities at and upstream of the vortex. The induced angle at the vortex decreases rapidly as the vortex moves downstream from about $\xi_1 = 1.0$, and is $\frac{\Gamma^1}{4}$ in the plane of the exit ($\xi_1 = 1.5$).

Closed-open-closed tunnel with one exit lip. Figure 19 shows results for a tunnel similar to that just discussed except that one exit lip is omitted. The two curves shown are very similar to the corresponding curves for the symmetrical condition. As was pointed out earlier, the horizontal component of the induced velocity on the axis is not zero for this unsymmetrical configuration. Values of this horizontal component have been plotted in figure 20 for the same two vortex locations as in figure 19. The values are seen to be very small in the forward part of the tunnel but become quite large in the neighborhood of the exit lip. The effect is consistent with the concept of the exit lip as a concentration of vortices having total strength equal and opposite to that of the bound vortex and serving thereby to turn the air back to its original direction. The fact that the two curves are practically identical lends further support to this viewpoint.

Comparison of the three tunnel types.— In figure 21 are compared the induced-angle curves for $\S_1=0.5$ and 1.0 for the three tunnel types just discussed. It is seen that the differences are slight up to about $\S=1.0$; beyond this value the curves for the closed-open tunnel continue to rise, while the others descend rapidly. The effect of the closed exit is somewhat larger for the tunnel with two exit lips than for the tunnel with one exit lip. Although the induced angles become slightly negative in the downstream closed region they eventually return to zero.

Symmetrical closed-open-closed tunnel with unequal pressures on the two free surfaces. By means of equation (24) calculations were made of the induced vertical velocities on the axis of a closed-open-closed tunnel of jet length equal to 1.5 times the tunnel height and having equal and opposite horizontal perturbation velocities (-ub and ub) on the upper and lower free surfaces, respectively. The results are plotted in figure 22. The curve shows that the vertical velocity component (or the induced angle) has an almost linear variation along the axis, which corresponds to the fairly uniform curvature of the jet that would be expected to result from the pressure difference between the upper and lower surfaces. For this same condition, the integral of the normal velocity along the free surface (equation (25)), which is the downward displacement of the jet boundary at the exit lip, was found to be 3.89ub.

For a vortex Γ' located at $\S_1 = 0.5$ in the equal-pressure case, the integral of the normal velocity along the free surface (equation (21)), which is proportional to the upward displacement of the jet boundary at the exit lip, was found to be 1.20r'. Accordingly, zero displacement at the exit, corresponding to the existence of a closed space above or below the jet (reference 2), will result if the flow described in the preceding paragraph is superposed on the equal-pressure flow in such proportion that $3.89u_b = 1.20\Gamma'$; that is, $\frac{u_b}{r!} = 0.31$. The corresponding effect on the induced angle at $\xi = \xi_1$ is found as follows: at $\xi = \xi_1 = 0.5$, $\frac{V}{\Gamma}$ for the equal-pressure case (fig. 18) is 0.48. From figure 22, $\frac{v}{v_b}$ at $\xi = 0.5$ for the unequal-pressure case is -1.44. Since $0.31 \times -1.44 = -0.45$, it is seen that, if spillage at the exit lip is prevented, the induced velocity in the region of the vortex is nearly eliminated. A similar comparison of the slopes of the curves in figures 18 and 22 in the neighborhood of \$ = 0.5 shows that the induced curvature in the region of the vortex is also nearly eliminated.

Résumé of numerical results. The induced angle at the lifting vortex is essentially that for an infinite open jet if the vortex is more than half the tunnel height from the entrance and the exit. The induced angles for case 2 (one fixed exit boundary) are nearly the same as for case 3 (symmetrical exit), so that any failure of the flow to contact the upper exit lip should not appreciably affect the tunnel correction. Finally, for case 3, if enough of the different-pressure flow is added to assure zero displacement of the free boundary at the exit (that is, if spillage at the exit is prevented, as by enclosing the space into which the spillage would normally occur), the induced angle at the vortex may be nearly eliminated.

III - CIRCULAR TUNNELS

In part III an outline is given of a general method for calculating the boundary effect in an open circular tunnel of finite jet length. The solution, involving expansions in Bessel functions, is somewhat similar to the solution for a closed circular tunnel (reference 13), but is constructed so that it satisfies the condition of uniformity of pressure over the open boundary and also the condition of continuity of velocity at the entrance lip. Numerical results are given for a lifting element on the tunnel axis.

SYMBOLS

ξ, η, ζ	rectangular coordinates in units of the tunnel radius with origin at lifting element (see fig. 23)
ξ, ρ, θ	cylindrical coordinates (see fig. 23)
a, b	\$-coordinate of entrance and exit lips, respectively
β	variable of integration
g	variable of integration (see reference 13)
ΦΟ	disturbance potential associated with body (or with vortex system)
Φ	tunnel-induced potential
$\Phi_{ m C}$	tunnel-induced potential in closed circular tunnel
Φ_{A}	residual potential $(\Phi - \Phi_C)$
J _m	Bessel function of the first kind of order m
u	constant longitudinal perturbation velocity on free surface
g _m (1)(ξ)	m th Fourier sine coefficient of $\frac{\partial \Phi_{A}}{\partial \rho}\Big _{\rho=1}$
g _m ⁽²⁾ (ξ)	m th Fourier cosine coefficient of $\frac{\partial \Phi_{A}}{\partial \rho}$ $\rho=1$
h _{mn} (j)	n th coefficient in series for g _m (j)(ξ)
y _{sm}	sth zero of Jm' (not including the zero at the origin)
r _m (1)	m th Fourier sine coefficient of $-\frac{\partial(\Phi_0 + \Phi_C)}{\partial \xi}\Big _{\rho=1}$
r _m (2)	m th Fourier cosine coefficient of $-\frac{\partial(\Phi_0 + \Phi_0)}{\partial \xi}$ $\rho=1$
δ	tunnel-induced velocity parameter $\left(\frac{w}{v} \frac{\pi R^2 \rho V^2}{2L}\right)$

ρ density of fluid

L lift of lifting element

w tunnel-induced velocity normal to the ξη-plane

V free-stream velocity

R tunnel radius

ANALYSIS

Introduction

In the analysis of the three-dimensional, circular, closed-open-closed tunnel, an appreciable simplification results when the tunnel axis lies in the plane of the horseshoe vortex. For off-center locations of the horseshoe vortex, or for a source-sink body on the axis, or for the general unsymmetrical disturbance, certain complications arise that are related to the fact that the pressure on the free boundary is then not equal to the pressure at $\pm\infty$ in the closed parts of the tunnel. That is, for these cases, if the net perturbation velocity is zero far upstream and downstream in the closed parts of the tunnel, a constant longitudinal perturbation velocity u \neq 0 will exist on the free surface. (See parts I and II.) A similar complication results for a source in a completely closed tunnel.

The analysis described in the following section is applicable directly to the case in which the tunnel axis lies in the plane of the horseshoe vortex and for which the longitudinal perturbation velocity on the free surface is zero. (See part I.) In the succeeding section are derived the additional terms needed for the solution of the more general problem. The significance of the titles of these two sections will become clear in the analysis.

Cylindrically Symmetric Term Omitted

Boundary conditions and formal expression for Φ_A . The solution is developed in cylindrical coordinates (ξ,ρ,θ) where the ξ -axis coincides with the tunnel axis and θ is measured from the horizontal plane. The relations of these coordinates to the rectangular coordinates (ξ,η,ζ) are indicated in figure 23. The distance variables ξ,η,ζ , and ρ are considered in units of the tunnel radius.

Let $\Phi_0(\xi,\rho,\theta)$ be the disturbance velocity potential associated with the lifting body in unlimited space (in particular, the velocity

potential of a horseshoe vortex). It is desired to find a function $\Phi(\xi, \rho, \theta)$, harmonic inside the cylinder $\rho = 1$, for which (see part I)

$$\frac{\partial (\Phi_0 + \Phi)}{\partial \rho} \bigg|_{\rho=1} = 0 \qquad (\xi < a, \xi > b)$$

$$\frac{\partial (\Phi_0 + \Phi)}{\partial \xi} \bigg|_{\rho = 1} = 0 \qquad (a < \xi < b)$$

where the region $\xi < a$, $\xi > b$ is the closed portion of the tunnel and a $< \xi < b$ is the open portion of the tunnel. In addition, according to the condition of continuity at the entrance lip (part I), the

derivative $\frac{\partial \Phi}{\partial \rho}\Big|_{\rho=1}$ must be continuous at $\xi = a$. The function Φ is

then the velocity potential of the additional flow due to the tunnel boundary.

The function of is conveniently considered in two parts:

$$\Phi = \Phi_{C} + \Phi_{A}$$

where Φ_{C} is the known tunnel-induced potential for the same vortex system in a completely closed circular tunnel (reference 13). The determining conditions for Φ_A are then

$$(1) \qquad \triangle \Phi_{\mathsf{A}} = 0 \qquad (\rho < 1)$$

(1)
$$\Delta \Phi_{A} = 0$$
 $(\rho < 1)$
(2) $\frac{\partial \Phi_{A}}{\partial \rho} = 0$ $(\xi < a, \xi > b)$

(3)
$$\frac{\partial \Phi_{\mathbf{A}}}{\partial \xi}\Big|_{\rho=1} = -\frac{\partial (\Phi_{\mathbf{O}} + \Phi_{\mathbf{C}})}{\partial \xi}\Big|_{\rho=1} \qquad (a < \xi < b)$$

$$\frac{\partial \Phi_{\mathbf{A}}}{\partial \rho} = 0 \qquad (\xi = \mathbf{a})$$

The function Φ_A may be expressed formally (see reference 13) as

$$\Phi_{A} = \sum_{m=1}^{\infty} \left[\sin m\theta \frac{1}{\pi} \int_{0}^{\infty} \frac{J_{m}(i\rho q)}{iqJ_{m}(iq)} dq \int_{a}^{b} g_{m}(1)(\beta) \cos q(\beta - \xi) d\beta \right]$$

+
$$\cos m\theta \frac{1}{\pi} \int_{0}^{\infty} \frac{J_{m}(i\rho q)}{iqJ_{m}(iq)} dq \int_{a}^{b} g_{m}(2)(\beta) \cos q(\beta - \xi) d\beta$$
 (26)

where $g_m^{(1)}(\xi)$ and $g_m^{(2)}(\xi)$ are, respectively, the mth sine and cosine coefficients of the Fourier series for $\frac{\partial \Phi_A}{\partial \rho}$ and q and β

are variables of integration. The integrations over β would, in general, have the range $-\infty$ to $+\infty;$ however, condition (2) shows that the functions $g_m^{~(j)}(\beta),~j=1,2,$ are zero from $-\infty$ to a and from b to $+\infty.$ The convergence of this function and its derivatives to the desired function Φ_A and its derivatives is discussed in the appendix of reference 13. A modification is necessary because of the discontinuity in $\frac{\partial \Phi_A}{\partial \rho}$ that may exist at $\xi=b$. For this case, the desired

convergence may be proved for regions bounded away from the circle $\rho=1$, $\xi=b$.

The assumption of zero perturbation velocity on the surface of the jet is equivalent to the assumption that the expansion of $-\frac{\partial (\Phi_0 + \Phi_C)}{\partial \xi}\Big|_{\rho=1}$ in a Fourier series in θ contains no term independent of θ . For this reason no m = 0 term appears in expansion (26). The next section discusses the somewhat special treatment that is required when the Fourier series contains a term independent of θ .

Evaluation of $g_m^{(j)}(\xi)$. The function Φ_A given in the preceding equation satisfies conditions (1) and (2) regardless of the precise form of the functions $g_m^{(j)}(\xi)$. It is now desired to find the functions $g_m^{(j)}(\xi)$ for a $<\xi<$ b such that Φ_A will satisfy conditions (3) and (4). To this end the functions are represented by infinite series of the form

$$g_{\text{m}}(j)(\xi) = h_{\text{m0}}(j) \sin \frac{\pi}{2} \frac{\xi - a}{b - a} + \sum_{n=1}^{\infty} h_{\text{mn}}(j) \sin n\pi \frac{\xi - a}{b - a}$$
 (27)

Since $g_m^{(j)}(a)$ thereby equals zero, condition (4) is automatically satisfied. Values of $g_m^{(j)}(b)$ are here assumed to be finite, instead of infinite (see part I); the corresponding inaccuracy, however, is considered to exist mainly in the immediate region of the exit lip $(\xi=b,\rho=1)$.

Substituting this series in equation (26) gives

$$\Phi_{A} = \sum_{m=1}^{\infty} \sum_{n=0}^{\infty} \left[h_{mn}^{(1)} P_{mn}(\xi, \rho) \sin m\theta + h_{mn}^{(2)} P_{mn}(\xi, \rho) \cos m\theta \right]$$
(28)

where

$$P_{mO}(\xi,\rho) = \frac{1}{\pi} \int_{0}^{\infty} \frac{J_{m}(i\rho q)}{iqJ_{m}(iq)} dq \int_{a}^{b} \sin \frac{\pi}{2} \frac{\beta - a}{b - a} \cos q(\beta - \xi) d\beta$$

and, for $n \neq 0$,

$$P_{mn}(\xi,\rho) = \frac{1}{\pi} \int_{0}^{\infty} \frac{J_{m}(i\rho q)}{iqJ_{m}(iq)} dq \int_{a}^{b} \sin n\pi \frac{\beta - a}{b - a} \cos q(\beta - \xi) d\beta$$

In the evaluation of these two expressions, the inner integrals may be found analytically and the outer integrals, which converge rapidly, may be found numerically. It is possible, however, by means of contour integration similar to that discussed in reference 14, to transform the infinite integrals into infinite series that are more convenient for the present purpose. The contour integration and the resulting infinite series are given in appendix A.

Differentiating equation (28) with respect to ξ and taking $\rho=1$ gives

$$\frac{\partial \Phi_{A}}{\partial \xi} \bigg|_{\rho=1} = \sum_{m=1}^{\infty} \sum_{n=0}^{\infty} \left[h_{mn}^{(1)} \sin m\theta \frac{\partial P_{mn}(\xi,1)}{\partial \xi} + h_{mn}^{(2)} \cos m\theta \frac{\partial P_{mn}(\xi,1)}{\partial \xi} \right]$$

$$(29)$$

The constants h_{mn} (j) are to be determined so that condition (3) is satisfied. For this purpose the function $-\frac{\partial (\Phi_0 + \Phi_C)}{\partial \xi}$ is expanded in a Fourier series in θ :

$$-\frac{\partial(\Phi_0 + \Phi_C)}{\partial \xi}\Big|_{\rho=1} = \sum_{m=1}^{\infty} \left[r_m^{(1)}(\xi) \sin m\theta + r_m^{(2)}(\xi) \cos m\theta \right]$$
 (30)

Equating coefficients in equations (29) and (30) in order to satisfy condition (3) then gives

$$r_{m}(j)(\xi) = \sum_{n=0}^{\infty} h_{mn}(j) \frac{\partial P_{mn}(\xi, 1)}{\partial \xi} \qquad (j = 1, 2)$$

It is assumed that the functions $r_m^{(j)}(\xi)$ can be satisfactorily approximated by a finite number of terms of these series. This assumption seems reasonable, inasmuch as $\frac{\partial P_{mm}(\xi,l)}{\partial \xi}$ is bounded as n approaches infinity (see appendix B) and $h_{mm}^{(j)}$ approaches zero as n approaches infinity. Thus,

$$r_{m}^{(j)}(\xi) \approx \sum_{n=0}^{N} h_{mn}(j) \frac{\partial P_{mn}(\xi, 1)}{\partial \xi}$$

The functions $r_m^{(j)}(\xi)$ and $\frac{\partial P_{mn}(\xi,1)}{\partial \xi}$ are computed at a set of points $\{\xi_i\}$, $i=0,1,2,\cdots$, where $i\geq N$. The coefficients $h_{mn}(j)$ are then determined (method of least squares) so that the expression

$$\sum_{i=0}^{I} \left[r_{m}(j)(\xi_{i}) - \sum_{n=0}^{N} h_{mn}(j) \frac{\partial P_{mn}(\xi_{i}, 1)}{\partial \xi} \right]^{2}$$

is a minimum for all values of $\, m \,$ and $\, j \cdot \,$ For each pair of values of $\, m \,$ and $\, j \cdot \,$ this condition gives $\, N \, + \, l \,$ equations for the $\, N \, + \, l \,$

unknowns $h_{m0}(j)$, $h_{m1}(j)$... $h_{mN}(j)$, as the N + 1 partial derivatives with respect to $h_{mn}(j)$ must be equal to zero. These equations are

$$\sum_{i=0}^{I} \left[r_{m}(j)(\xi_{i}) \frac{\partial P_{mk}(\xi_{i},1)}{\partial \xi} - \sum_{n=0}^{N} h_{mn}(j) \frac{\partial P_{mn}(\xi_{i},1)}{\partial \xi} \frac{\partial P_{mk}(\xi_{i},1)}{\partial \xi} \right] = 0$$

$$(k = 0, 1, 2, \dots N)$$

Remarks on the computations. The points $\{\xi_i\}$ and the value of N are chosen so that the addition of more points and increasing the value of N will no longer appreciably affect the results. It is clear that the point $\xi = b$ cannot be used and that care must be taken not to choose too large a proportion of the points $\{\xi_i\}$ in the neighborhood of $\xi = a$ and $\xi = b$; any such attempt to describe more accurately the infinite values of $g_m(j)(\xi)$ at $\xi = b$ or of its derivatives at $\xi = a$ and $\xi = b$ with a finite number of coefficients will cause a large error in the approximations to $g_m(\xi)$ elsewhere in the interval $a < \xi < b$.

Since the functions $r_m^{(j)}(\xi)$ rapidly approach zero as m approaches infinity, the preceding equations need be solved for only a small number of values of m. The values of $h_{mn}^{(j)}$ thus obtained can be used to give an approximation to the function Φ_A (equation (28)):

$$\Phi_{A} = \sum_{m=1}^{M} \sum_{n=0}^{N} \left[h_{mn}^{(1)} P_{mn}(\xi, \rho) \sin m\theta + h_{mn}^{(2)} P_{mn}(\xi, \rho) \cos m\theta \right]$$
(31)

Any desired interference velocity may now be obtained by differentiating this series term by term and adding the results to the corresponding interference velocity for the closed tunnel.

The vertical induced velocity in the plane of symmetry is simply

$$\frac{\partial \Phi_{A}}{\partial \zeta}\Big|_{\zeta=0} = \frac{1}{\rho} \frac{\partial \Phi_{A}}{\partial \theta}\Big|_{\theta=0}$$

for points on the right side of the tunnel axis, or

$$\frac{\partial \Phi_{A}}{\partial \zeta}\Big|_{\zeta=0} = -\frac{1}{\rho} \frac{\partial \Phi_{A}}{\partial \theta}\Big|_{\theta=\pi}$$

for points on the left side of the tunnel axis. Inspection of equation (31)

shows immediately that the θ -derivative of the second term in the bracket is zero for either case and the contribution of the first term is

$$\frac{1}{\rho} \frac{\partial \Phi_{A}}{\partial \theta} \Big|_{\theta=0} = \frac{1}{\rho} \sum_{m=1}^{M} \sum_{n=0}^{N} mh_{mn}(1) P_{mn}(\xi,\rho)$$

or

$$-\frac{1}{\rho}\frac{\partial \Phi_{A}}{\partial \theta}\bigg|_{\theta=\pi} = -\frac{1}{\rho}\sum_{m=1}^{M}\sum_{n=0}^{N} (-1)^{m} mh_{mn}^{(1)} P_{mn}(\xi,\rho)$$

Furthermore, all vertical velocities on the axis itself may be obtained by considering only m = 1, because

$$\lim_{\rho \to 0} \frac{1}{\rho} P_{mn}(\xi, \rho) \equiv 0 \qquad (m > 1)$$

The usual geometric symmetries also contribute toward simplifying the calculations. For example, if the horseshoe vortex lies in the horizontal plane of symmetry of the tunnel,

$$g_m(2) = r_m(2) = h_{mn}(2) = 0$$

If, in addition, the vertical plane of symmetry of the tunnel is also the vertical plane of symmetry of the horseshoe vortex, all even values of m are eliminated; in the corresponding antisymmetrical case (as with aileron deflection) all odd values of m are eliminated.

Cylindrically Symmetric Term

For a normal velocity at the tunnel wall $g_0(\xi)$ that is independent of θ the potential function cannot be given exactly in the form of the preceding section since for m=0 the integral with respect to q will, in general, not converge for q in the neighborhood of zero. It is necessary to add additional terms to the potential so as to insure the convergence of the integrals with respect to q. Moreover, these terms must be of such a nature that the potential function is still harmonic and gives the required normal velocity at the tunnel wall.

The singularity-free potential inside the tunnel then takes the form

$$\Phi = \frac{1}{\pi} \int_{0}^{\infty} \left[\frac{J_{0}(i\rho q)}{iqJ_{0}(iq)} \int_{-\infty}^{\infty} g_{0}(\beta) \cos q(\beta - \xi) d\beta \right]$$

$$-\frac{2\pi k\xi}{q} - \frac{2}{q^2} \int_{-\infty}^{\infty} g_0(\beta) d\beta d\beta$$

where $k = \lim_{|\beta| \to \infty} \frac{g_0(\beta)}{\beta}$ and where $\int_{-\infty}^{\infty} g_0(\beta) d\beta$ is the Cauchy principal

value of the integral. Both the limit and the integral must be assumed to exist.

The appearance of these additional terms is not wholly due to the presence of the open section in the tunnel. For a source in a completely closed tunnel the second term does not vanish and would have to be used in calculating the tunnel-induced perturbation velocity by the method of reference 13. However, for a closed body or a vortex system plus its reflections in a completely closed tunnel, both of these additional terms vanish.

It is easy to verify the fact that the additional terms do insure the convergence of the integral with respect to q. A straightforward differentiation then shows that Φ is in fact harmonic and satisfies the boundary condition $\frac{\partial \Phi}{\partial \rho} = g_0(\xi)$.

For the closed-open-closed tunnel, the boundary condition (see part I) that the velocities far upstream and downstream be equal is no longer automatically satisfied by putting the total tangential velocity on the jet surface equal to zero. The determining conditions for $\Phi_{\rm A}$ are now

$$(1) \qquad \triangle \Phi_{A} = 0 \qquad (\rho < 1)$$

(2)
$$\frac{\partial \Phi_{\mathbf{A}}}{\partial \rho}\Big|_{\rho=1} = 0$$
 ($\xi < a \text{ and } \xi > b$)

(3)
$$\frac{\partial \Phi_{A}}{\partial \xi}\Big|_{\rho=1} = -\frac{\partial (\Phi_{O} + \Phi_{C})}{\partial \xi}\Big|_{\rho=1} + u \qquad (a \leq \xi < b)$$

(4)
$$\lim_{\xi \to +\infty} \frac{\partial^{\Phi} A}{\partial^{\xi}} = \lim_{\xi \to -\infty} \frac{\partial^{\Phi} A}{\partial^{\xi}}$$

(5)
$$\frac{\partial \Phi_{\mathbf{A}}}{\partial \rho}\Big|_{\rho=1} = 0 \qquad (\xi = \mathbf{a})$$

Conditions (1) and (2) are satisfied by assuming $g_0(\xi) = 0$ for $\xi < a$ and $\xi > b$. Thus

$$\Phi_{A} = \frac{1}{\pi} \int_{0}^{\infty} \left[\frac{J_{O}(i\rho q)}{iqJ_{O}(iq)} \int_{a}^{b} g_{O}(\beta) \cos q(\beta - \xi) d\beta - \frac{2}{q^{2}} \int_{a}^{b} g_{O}(\beta) d\beta \right] dq$$
 (32)

Again it is desired to find $g_0(\xi)$ for a < ξ < b so that ϕ_A will satisfy conditions (3), (4), and (5). The representation of $g_0(\xi)$ in the same form as before (equation 27)

$$g_0(\xi) = h_{00} \sin \frac{\pi}{2} \frac{\xi - a}{b - a} + \sum_{n=1}^{\infty} h_{0n} \sin n\pi \frac{\xi - a}{b - a}$$

automatically satisfies condition (5). Substituting this series in equation (32) gives

$$\Phi_{A} = \sum_{n=0}^{\infty} h_{On} P_{On}(\xi, \rho)$$

where

$$P_{OO}(\xi,\rho) = \frac{1}{\pi} \int_{0}^{\infty} \left[\frac{J_{O}(i\rho q)}{iqJ_{O}(iq)} \int_{a}^{b} \sin \frac{\pi}{2} \frac{\beta - a}{b - a} \cos q(\beta - \xi) d\beta \right]$$

$$-\frac{2}{q^2}\int_a^b \sin\frac{\pi}{2}\frac{\beta-a}{b-a}d\beta dq$$

$$\begin{split} P_{On}(\xi,\rho) &= \frac{1}{\pi} \int_0^\infty \!\! \left[\frac{J_O(\mathrm{i}\rho q)}{\mathrm{i}qJ_O'(\mathrm{i}q)} \! \int_a^b \sin n\pi \frac{\beta-a}{b-a} \cos q(\beta-\xi) \, \mathrm{d}\beta \right. \\ &\left. - \frac{2}{q^2} \int_a^b \sin n\pi \frac{\beta-a}{b-a} \, \mathrm{d}\beta \right] \mathrm{d}q \end{split}$$

The resulting infinite series for the $P_{On}(\xi,\rho)$ obtained by means of contour integrations are given in appendix A.

Condition (3) then becomes

$$\sum_{n=0}^{\infty} h_{0n} \frac{\partial P_{0n}(\xi, 1)}{\partial \xi} = -\frac{\partial (\Phi_0 + \Phi_C)}{\partial \xi} + u \qquad (a \leq \xi < b)$$

But (see appendix A)
$$\lim_{\xi \to +\infty} \frac{\partial P_{On}}{\partial \xi} = -\lim_{\xi \to -\infty} \frac{\partial P_{On}}{\partial \xi}$$

and so $\lim_{\xi \to +\infty} \frac{\partial \Phi_{A}}{\partial \xi} = -\lim_{\xi \to -\infty} \frac{\partial \Phi_{A}}{\partial \xi}$ so that condition (4) becomes

 $\lim_{\xi \to +\infty} \frac{\partial \Phi_A}{\partial \xi} = 0.$ Thus it is necessary that

$$\frac{h_{00}}{\frac{\pi}{2(b-a)}} + \frac{\frac{\infty}{h_{0n}} \left[1 - (-1)^{n}\right]}{\frac{n\pi}{b-a}} = 0$$

There exists a unique value of u for which the coefficients hon will satisfy this equation and it can be found as follows: Let

$$h_{On} = h_{On}' + uh_{On}''$$

where

$$\sum_{n=0}^{\infty} h_{0n}' \frac{\partial P_{0n}(\xi,1)}{\partial \xi} = -\frac{\partial (\Phi_0 + \Phi_C)}{\partial \xi} \Big|_{\rho=1}$$

and

$$\sum_{n=0}^{\infty} h_{0n} \frac{\partial P_{0n}(\xi,1)}{\partial \xi} = 1$$

then if

$$\frac{h_{00}' + uh_{00}''}{\frac{\pi}{2(b-a)}} + \sum_{n=1}^{\infty} \frac{\left(h_{0n}' + uh_{0n}''\right) \left[1 - (-1)^n\right]}{\frac{n\pi}{b-a}} = 0$$

$$u = -\frac{2h_{00}' + \sum_{n=1}^{\infty} \frac{h_{0n}'}{n} \left[1 - (-1)^n\right]}{2h_{00}'' + \sum_{n=1}^{\infty} \frac{h_{0n}''}{n} \left[1 - (-1)^n\right]}$$

The coefficients h_{0n} and h_{0n} are found by solution of sets of simultaneous linear equations, as described in the previous section.

The function Φ_A '' = $\sum h_{On}$ ''P_{On}(ξ , ρ) is the perturbation potential which, when added to that of a uniform flow, gives the potential of the disturbance-free expanding tunnel described in part I and indicated in figure 2. The corresponding perturbation velocities $\frac{\partial \Phi_A}{\partial \xi}$ have equal and opposite values at ∞ and $-\infty$.

EXAMPLE

As a somewhat simplified illustration, the problem of a semiinfinite unit doublet distribution (degenerate horseshoe vortex) along
the tunnel axis was considered. The tunnel was assumed to have an open
jet, 3 tunnel radii in length. The tunnel interference was calculated
for four different positions of the upstream end of the doublet distribution, these positions being 0.1, 0.4, 0.7, and 1.0 radii downstream
from the entrance. If the upstream end is taken as the origin of the
coordinate system, then (see appendix C)

$$r_1^{(1)}(\xi) = -\frac{1}{(1+\xi^2)^{3/2}} - \frac{2}{\pi} \int_0^{\infty} \frac{J_1(iq)}{iJ_1(iq)} \left[qK_0(q) + K_1(q) \right] \cos q\xi \, dq$$

$$r_{\rm m}^{(j)}(\xi) \equiv 0 \qquad (m \neq 1, j \neq 1)$$
 (33)

where Ko and K1 are the Bessel functions as defined in reference 15.

The points $\{\xi_i\}$ were taken as a, a + 0.3, a + 0.6, . . . a + 2.7, that is, a set of ten points, at 0.3 intervals, starting with the entrance lip of the tunnel. The coefficients $h_{ln}(1)$ were found by the method of least squares for $N=0, 1, \cdots, 5$ and also so as to satisfy the equations $r_1(1)(\xi_i)=\sum_{n=0}^{\infty}h_{ln}(1)\frac{\partial P_{ln}(\xi,1)}{\partial \xi}$ at all ten points. Plots of the resulting functions $g_1(1)(\xi)$ for the different values of N indicated that convergence was essentially complete for N between 3 and 5. This simplification results in appreciable saving in the amount of computation. Not only is it necessary to solve a smaller set of simultaneous equations, but also P_{ln} and $\partial P_{ln}/\partial \xi$ need be found for fewer values of n.

The computation was fairly straightforward. In the determination of $r_1^{(1)}(\xi)$, K_0 and K_1 were obtained from the tables of reference 15, and J_1 and J_1' from the tables and from the relations between the Bessel functions and their derivatives (references 15 and 16). Weddle's formula (reference 17) is convenient for performing the integrations. In the case of P_{1n} , the values of y_{s1} appearing in the formula for $Q_{1n}(s)(\rho)$ were found from the formula in appendix III of reference 15, and J_1 and J_1' as just noted. In the evaluation of $\lim_{\rho \to 0} \frac{1}{\rho} P_{1n}$ it is noted that the value of $\lim_{\kappa \to 0} \frac{1}{\kappa} J_1(\kappa) = \frac{1}{2}$.

The results of these computations, together with those for the completely open and completely closed tunnels and those given in reference 3 are shown in figures 24, 25, and 26. In figure 24, the vertical tunnel-induced velocity along the axis for the four different positions of the lifting element together with the results for the open and closed tunnels are plotted against distance from the lifting element. The same results are plotted against the longitudinal distance from the entrance lip in figure 25. Figure 26 shows the results of reference 3 compared with the results of this paper for the same case - that of the lifting element 1 radius downstream from the entrance lip.

The tunnel-induced velocity in the upstream regions and in the neighborhood of the lifting element, although only slightly less than that for an open tunnel for the lifting element 1 radius downstream, falls off more and more rapidly as the lifting element is moved towards the entrance lip. The maximum induced velocity is attained about 1 radius upstream from the exit, and is never more than 78 percent of the maximum value for a completely open tunnel. After the maximum the values fall rapidly and approach the values for a closed tunnel in the downstream regions. The results of reference 3 (see fig. 26) are consistently below the present results especially in the region behind the lifting element.

An extrapolation from the present results indicates that the induced upflow at the lifting element, for the lifting element in the plane of the entrance lip, is approximately zero, or the average between the completely open and completely closed cases. The same result (that the effect in the plane of the entrance lip is the average of the effects for the completely open and the completely closed tunnels) was also obtained for the two-dimensional tunnel (fig. 18).

CONCLUSION

For an open wind tunnel, the corrections corresponding to an infinitely long open jet will usually be adequately accurate if the region of interest (where the lift is located and where the boundary-induced flow is being considered) is at least half the jet height from the jet entrance and exit sections. As the distance of the lifting element from the entrance is decreased below this limit, the boundary-induced flow decreases rapidly and, when the lifting element is in the entrance plane, the induced angle at the lifting element is about the average of that for an open tunnel and that for a closed tunnel.

In the theoretical studies of these flows, the usual boundary conditions of pressure uniformity on the free surface and of zero normal velocity on the closed surface must be supplemented with the conditions that the velocity be continuous at the entrance lip and that the velocities far downstream and far upstream in the closed sections be equal. For the two-dimensional open tunnel, a convenient general mathematical approach is to transform the infinite strip (representing the tunnel) to the upper half-plane by the logarithmic transformation and then to develop the desired complex velocity in this transformed plane. For the circular open tunnel the solution may be effected by expressing the potential by a finite series of Bessel functions, satisfying the boundary condition on the free surface at a finite number of points, and solving for the coefficients by simultaneous linear equations.

For noncircular open wind tunnels, solutions in terms of available functions will be very inconvenient. For such cases, the trends indicated by the present results may suffice, when applied to the presumably known corrections for the infinitely long open and closed configurations, to provide adequate corrections. Solutions for the general three-dimensional configuration may also be possible by electrical-analogy methods, in which either the perturbation velocity potential or the acceleration potential is analogous to the electrical potential in an electrolyte solution. Such analogies may be characterized, however, by considerable technical difficulty.

APPENDIX A

EVALUATION OF Pmn(\$,0)

Evaluation for $m \neq 0$

Contour integration -- For $n \neq 0$,

$$P_{mn}(\xi,\rho) = \frac{1}{\pi} \int_{0}^{\infty} \frac{J_{m}(i\rho q)}{iqJ_{m}(iq)} dq \int_{a}^{b} \sin n\pi \frac{\beta - a}{b - a} \cos q(\beta - \xi) d\beta$$
 (Al)

The inner integral may be found directly:

$$\int_{a}^{b} \sin n\pi \frac{\beta - a}{b - a} \cos q(\beta - \xi) d\beta$$

$$=\frac{1}{2}\int_{a}^{b}\left\{\sin\left[nr\frac{\beta-a}{b-a}+q(\beta-\xi)\right]+\sin\left[nr\frac{\beta-a}{b-a}-q(\beta-\xi)\right]\right\}d\beta$$

$$= \frac{\frac{n\pi}{b-a}}{q^2 - \left(\frac{n\pi}{b-a}\right)^2} \left[(-1)^n \cos q(b-\xi) - \cos q(\xi-a) \right]$$
 (A2)

The problem of evaluating $P_{mn}(\xi,\rho)$ thus reduces to that of evaluating integrals of the form

$$\int_0^\infty \frac{J_m(ipq) \cos kq \, dq}{iqJ_m'(iq)(q^2 - h^2)}$$

Consider the integral in the complex z-plane

$$\frac{1}{2\pi i} \oint \frac{J_{m}(i\rho z) e^{ikz}}{iz J_{m}'(iz) (z^{2} - h^{2})} dz$$

around the contour indicated in figure 27. Its value is the sum of the residues of the integrand at its poles inside the contour. These poles are the values of z for which $J_m'(iz) = 0$. The zeros of J_m' will be designated y_{sm} ; they are real and may be obtained from the formula in appendix III of reference 15. The poles of the integrand then occur at $iz = y_{sm}$, that is, at $z = -iy_{sm}$. Since only the poles within the contour are desired, only the negative zeros of J_m' are considered.

The residue of $\frac{1}{J_m'(iz)}$ at $z = -iy_{sm}$ is,

$$\lim_{z \to -iy_{sm}} \frac{z + iy_{sm}}{J_{m}'(iz)} = \lim_{z \to -iy_{sm}} \frac{z + iy_{sm}}{J_{m}'(iz) - J_{m}'(y_{sm})}$$

since $J_m'(y_{sm}) = 0$; by the definition of the derivative this expression reduces to

$$-\frac{1}{J_{m}^{11}(y_{sm})}$$

The residue of the integrand at $z = -iy_{sm}$ is thus

$$i\frac{J_m(\rho y_{sm})e^{ky_{sm}}}{y_{sm}(y_{sm}^2 + h^2)J_m''(y_{sm})}$$

But the Bessel functions satisfy the relation

$$J_{m}'' + \frac{1}{x}J_{m}' + \left(1 - \frac{m^{2}}{x^{2}}\right)J_{m} = 0$$

so that at $x = y_{sm}$, where $J_m' = 0$,

$$J_{m}''(y_{sm}) = \frac{m^2 - y_{sm}^2}{y_{sm}^2} J_{m}(y_{sm})$$

whence, finally,

$$\frac{1}{2\pi i} \oint \frac{J_{\text{m}}(i\rho z)e^{ikz} dz}{izJ_{\text{m}}!(iz)\begin{pmatrix} 2 & 2 \\ z & -h \end{pmatrix}} = i \underbrace{\int \frac{J_{\text{m}}(\rho y_{\text{sm}})e^{ky_{\text{sm}}}y_{\text{sm}}}{2 \begin{pmatrix} 2 & 2 \\ y_{\text{sm}} & +h \end{pmatrix} \begin{pmatrix} 2 & 2 \\ m & -y_{\text{sm}} \end{pmatrix}}_{\text{m}} J_{\text{m}}(y_{\text{sm}})$$

where the number of terms in the summation depends on the radius of the outer semicircle.

For $k \ge 0$, if the radius of the outer semicircle is allowed to approach infinity in discrete steps so as to avoid the poles of the integrand, the integral over the semicircle approaches zero. The limiting values of the integrals along the two inner semicircles, as their radii approach zero, are readily determined by the usual process as

$$i\frac{J_m(-i\rho h)e^{-ikh}}{4h^2J_m'(-ih)}$$

and

$$i\frac{J_m(i\rho h)e^{ikh}}{4h^2J_m'(ih)}$$

These two terms may be combined, after noting that reversing the sign of the argument in J_m and J_m merely reverses the sign of their ratio, to

$$-\frac{J_{m}(i\rho h)}{2h^{2}J_{m}'(ih)}\sin kh$$

Equating the total integral along the infinite contour to the sum of the residues thus gives

$$\frac{1}{2\pi i} \int_{-\infty}^{\infty} \frac{J_m(i\rho q) e^{ikq} dq}{iq J_m'(iq) \left(q^2 - h^2\right)} = \frac{J_m(i\rho h)}{2h^2 J_m'(ih)} \sin kh$$

$$-i \sum_{s=0}^{\infty} \frac{J_m(\rho y_{sm}) e^{-ky_{sm}} y_{sm}}{\left(y_{sm}^2 + h^2\right) \left(m^2 - y_{sm}^2\right) J_m(y_{sm})}$$

where the y_{sm} terms are now defined as the positive zeros of J_m ' instead of the negative zeros (if J_m '(x) = 0, so also does J_m '(-x)). By equating the imaginary part of the left-hand term to the right-hand side, which is a pure imaginary, there results, finally

$$\int_0^\infty \frac{J_m(i\rho q) \cos kq \, dq}{iqJ_m'(iq)(q^2 - h^2)} = \frac{\pi iJ_m(i\rho h)}{2h^2J_m'(ih)} \sin kh$$

$$+ \pi \sum_{s=0}^{\infty} \frac{J_{m}(\rho y_{sm}) e^{-ky_{sm}} y_{sm}}{(y_{sm}^{2} + h^{2})(m^{2} - y_{sm}^{2}) J_{m}(y_{sm})}$$

Expressions for P_{mn} , $n \neq 0$, $m \neq 0$. In the preceding development it was assumed that $k \geq 0$, which was acceptable with regard to equation (A2) in view of the fact that the cosine is an even function of the variable. This essentially nonnegative value of k must be retained, however, in the final expressions for $P_{mn}(\xi,\rho)$:

$$P_{mn} = -\frac{1}{2} \frac{J_m \left(i\rho \frac{n\pi}{b-a}\right)}{\frac{i}{b-a}J_m \left(i\frac{n\pi}{b-a}\right)} \left[(-1)^n \sin \frac{|b-\xi|n\pi}{b-a} - \sin \frac{|\xi-a|n\pi}{b-a} \right]$$

$$+ \frac{n\pi}{b-a} \sum_{s=0}^{\infty} \frac{J_m(\rho y_{sm})y_{sm}}{\left[\left(y_{sm}\right)^2 + \left(\frac{n\pi}{b-a}\right)^2\right] \left[m^2 - \left(y_{sm}\right)^2\right] J_m(y_{sm})} (-1)^{n_e - \left|b-\xi\right| y_{sm}}$$

$$- e^{-\left|\xi-a\right| y_{sm}}$$
(A3)

Now for $a \leq \xi \leq b$

$$(-1)^{n} \sin \frac{|b - \xi| n\pi}{b - a} = (-1)^{n} \sin \left[\frac{b - a - (\xi - a)}{b - a} n\pi \right]$$

$$= -\sin n\pi \frac{\xi - a}{b - a}$$

$$= -\sin n\pi \frac{|\xi - a|}{b - a}$$

For $\xi < a$,

$$(-1)^{n} \sin \frac{b - \xi \mid n\pi}{b - a} = -(-1)^{n} \sin \left[\frac{b - a + (a - \xi)}{b - a} n\pi \right]$$

$$= \sin n\pi \frac{a - \xi}{b - a}$$

$$= \sin n\pi \frac{|\xi - a|}{b - a}$$

For $\xi > b$,

$$(-1)^{n} \sin \frac{b-\xi n\pi}{b-a} = (-1)^{n} \sin \frac{\xi-a-(b-a)}{b-a} n\pi$$

$$= \sin n\pi \frac{\xi-a}{b-a}$$

$$= \sin n\pi \frac{\xi-a}{b-a}$$

The first term on the right-hand side of equation (A3) is thus equal to zero for $\xi < a$ or $\xi > b$. The desired expressions for $P_{mn}(\xi,\rho)$, $n \neq 0$, are therefore, for $a \leq \xi \leq b$,

$$\begin{split} P_{mn}(\xi,\rho) &= \frac{J_m \left(i\rho \frac{n\pi}{b-a}\right)}{i\frac{n\pi}{b-a}J_m! \left(i\frac{n\pi}{b-a}\right)} \sin n\pi \frac{\xi-a}{b-a} \\ &- \frac{n\pi}{b-a} \sum_{s=0}^{\infty} Q_{mn}(s)(\rho) \left[e^{-(\xi-a)y_{sm}} - (-1)^n e^{-(b-\xi)y_{sm}}\right] \end{split}$$

and, for $\xi \leq a$ or $\xi \geq b$,

$$P_{mn}(\xi,\rho) = -\frac{n\pi}{b-a} \sum_{s=0}^{\infty} Q_{mn}(s)(\rho) \left[e^{-|\xi-a|y_{sm}} - (-1)^{n} e^{-|b-\xi|y_{sm}} \right]$$

where

$$Q_{mn}(s) = \frac{J_{m}(\rho y_{sm})y_{sm}}{\left[y_{sm}^{2} + \left(\frac{n\pi}{b-a}\right)^{2}\right]\left(m^{2} - y_{sm}^{2}\right)J_{m}(y_{sm})}$$
 (n \neq 0)

The calculations for n=0, which follow similar lines, are not given here. The final formulas are, for $a \le \xi < b$,

$$P_{mO}(\xi,\rho) = \frac{J_{m}\left(i\rho\frac{\pi}{2(b-a)}\right)}{\frac{i\pi}{2(b-a)}J_{m}!\left(\frac{i\pi}{2(b-a)}\right)} \sin\frac{\pi}{2}\frac{\xi-a}{b-a}$$

+
$$\sum_{s=0}^{\infty} Q_{m0}(s)(\rho) \left[y_{sm} e^{-(b-\xi)y_{sm}} - \frac{\pi}{2(b-a)} e^{-(\xi-a)y_{sm}} \right]$$

for $\xi \leq a$,

$$P_{mO}(\xi,\rho) = \sum_{s=0}^{\infty} Q_{mO}(s)(\rho) \left[y_{sm} e^{-(b-\xi)y_{sm}} - \frac{\pi}{2(b-a)} e^{-(a-\xi)y_{sm}} \right]$$

and, for $\xi > b$,

$$P_{mO}(\xi,\rho) = -\sum_{s=0}^{\infty} Q_{mO}(s)(\rho) \left[y_{sm} e^{-(\xi-b)y_{sm}} + \frac{\pi}{2(b-a)} e^{-(\xi-a)y_{sm}} \right]$$

where

$$Q_{mO}(s)(\rho) = \frac{J_{m}(\rho y_{sm})y_{sm}}{\left\{y_{sm}^{2} + \left[\frac{\pi}{2(b-a)}\right]^{2}\right\}(m^{2} - y_{sm}^{2})J_{m}(y_{sm})}$$

Evaluation for m = 0

The evaluation of $P_{mn}(\xi,\rho)$ for m=0 proceeds essentially as before with the difference that the contour of integration must avoid the origin. For n=0, the final formulas are for $a<\xi< b$.

$$P_{00}(\xi,\rho) = -\frac{2(b-a)}{\pi}^{2} - \frac{\xi-a}{\frac{\pi}{2(b-a)}} + \frac{J_{0}[i\rho \frac{\pi}{2(b-a)}]}{\frac{i\pi}{2(b-a)}J_{0}[i \frac{\pi}{2(b-a)}]} \sin \frac{\pi}{2} \frac{\xi-a}{b-a}$$

$$+ \sum_{s=0}^{\infty} Q_{00}(s) \left[y_{s0} e^{-(b-\xi)} y_{s0} - \frac{\pi}{2(b-a)} e^{-(\xi-a)} y_{s0} \right]$$

for $\xi < a$,

$$P_{00}(\xi,\rho) = -\left[\frac{2(b-a)}{\pi}\right]^{2} + \frac{\xi-a}{\frac{\pi}{2(b-a)}} + \sum_{s=0}^{\infty} Q_{00}(s) \left[y_{s0}e^{-(b-\xi)}y_{s0} - \frac{\pi}{2(b-a)}e^{-(a-\xi)}y_{s0}\right]$$

and, for $\xi > b$,

$$P_{00}(\xi,\rho) = -\left[\frac{2(b-a)}{\pi}\right]^2 - \frac{\xi-a}{\frac{\pi}{2(b-a)}}$$

$$-\sum_{s=0}^{\infty} Q_{00}(s) \left[y_{s0}e^{-(\xi-b)}y_{s0} - \frac{\pi}{2(b-a)} e^{-(\xi-a)}y_{s0} \right]$$

For $n \neq 0$, the corresponding formulas are, for $a \leq \xi < b$,

$$P_{On}(\xi,\rho) = -\frac{1}{\frac{n\pi}{b-a}} \left[(\xi - a) - (-1)^n (b - \xi) \right]$$

$$+\frac{J_0\left(\mathrm{i}\rho\frac{n\pi}{b-a}\right)}{\frac{\mathrm{i}n\pi}{b-a}J_0!\left(\mathrm{i}\frac{n\pi}{b-a}\right)}\sin n\pi\frac{\xi-a}{b-a}$$

$$-\frac{n\pi}{b-a}\sum_{s=0}^{\infty}Q_{0n}(s)\left[e^{-(\xi-a)y_{s0}}-(-1)^{n_{e}^{-(b-\xi)}y_{s0}}\right]$$

for \$ < a,

$$P_{On}(\xi,\rho) = -\frac{1}{\frac{n\pi}{b-a}} [(a - \xi) - (-1)^n(b - \xi)]$$

$$-\frac{n\pi}{b-a}\sum_{s=0}^{\infty}Q_{0n}(s)\left[e^{-(a-\xi)y_{s0}}-(-1)^{n}e^{-(b-\xi)y_{s0}}\right]$$

and, for $\xi > b$,

$$P_{On}(\xi,\rho) = -\frac{1}{\frac{n\pi}{b-a}} [(\xi - a) - (-1)^n(\xi - b)]$$

$$-\frac{n\pi}{b-a} \sum_{s=0}^{\infty} Q_{0n}(s) \left[e^{-(\xi-a)y_{s0}} - (-1)^{n} e^{-(\xi-b)y_{s0}} \right]$$

APPENDIX B

PROOF THAT
$$\frac{\partial P_{mn}(\xi,1)}{\partial \xi}$$
 IS BOUNDED AS $n \to \infty$, $a \le \xi \le b$

Differentiating the formula from appendix A for $P_{mn}(\xi,\rho)$ and putting $\rho=1$ gives

$$\frac{\partial P_{mm}(\xi,1)}{\partial \xi} = \frac{J_m(\frac{1-n\pi}{b-a})}{iJ_m'(\frac{1-n\pi}{b-a})} \cos n\pi \frac{\xi-a}{b-a}$$

$$+ \frac{n\pi}{b-a} \sum_{s=0}^{\infty} \frac{y_{sm}^2}{\left[y_{sm}^2 + \left(\frac{n\pi}{b-a}\right)^2\right] \left(m^2 - y_{sm}^2\right)} \left[e^{-(\xi-a)y_{sm}}\right]$$

$$+ (-1)^n e^{-(b-\xi)y_{sm}}$$

The second term of the right-hand member is of order $\frac{1}{n}$ for large n so that

$$\lim_{n\longrightarrow\infty}\frac{\partial P_{mn}(\xi,1)}{\partial\xi}=\lim_{n\longrightarrow\infty}\frac{J_m\left(\frac{i-n\pi}{b-a}\right)}{iJ_m\left(\frac{i-n\pi}{b-a}\right)}\cos n\pi\frac{\xi-a}{b-a}$$

The cosine factor of this expression merely oscillates between 1 and -1. For the remaining factor, it is noted from the asymptotic expressions for the Bessel functions (reference 15, pp. 59-61) that $J_m(it)$ is essentially of the form $i\frac{m-e^t}{\sqrt{2\pi t}}$ as $t\to\infty$, from which it can be readily shown that the fraction $J_m(it)$ approaches unity as $t\to\infty$.

APPENDIX C

DERIVATION OF EQUATION (32)

Equation (32) was derived for use in calculating some of the results given in reference 13, but it was not explicitly stated and discussed in that paper. Because certain steps in its development are not obvious, the present outline of its derivation is given. Familiarity with reference 13 will be assumed.

Certain difficulties arise in the treatment of the doublet line directly; so the result is found by considering a horseshoe vortex of finite span and letting the span approach zero. Equation (6) of refer-

ence 13 gives the formula for $\frac{\partial \Phi_2}{\partial \rho}\Big|_{\rho=1}$ (where Φ_2 is defined in refer-

ence 13) corresponding to a horseshoe vortex of strength Γ and span σ having one trailing vortex along the tunnel axis and the other to the right of the axis. The procedure for the doublet consists of letting the yaw angle Ψ be zero, expanding the radicals in ascending powers of σ , and proceeding to the next step in the analysis, where σ will eventually be made to approach zero. In the expansions, powers of σ higher than the first may be neglected except where σ occurs in the product $\xi \sigma$, since ξ takes on infinite values; furthermore, since for the doublet the field should be symmetrical about the vertical plane of symmetry $\left(\theta = \frac{\pi}{2}\right)$, unsymmetrical factors, as $\sigma \cos \theta$, may be immediately eliminated. The formula for $\frac{\partial \Phi_2}{\partial \rho}$ is thus

$$\frac{\partial \Phi_{2}}{\partial \rho} \Big|_{\rho=1} = -\frac{P\sigma}{4\pi} \lim_{\sigma \to 0} \left\{ \sin \theta \left(\frac{\xi_{\sigma}}{\sqrt{1 + \xi^{2}\sigma^{2}}} - \frac{\xi}{\sqrt{1 + \xi^{2}}} \right) - \frac{\xi \sin \theta}{\sigma(\xi^{2} + \sin^{2}\theta)} \left(1 - \frac{1}{\sqrt{1 + \xi^{2}\sigma^{2}}} \right) - \frac{\xi \sin \theta}{\xi^{2} + \sin^{2}\theta} \left[\frac{1}{\sqrt{1 + \xi^{2}}} - \frac{\cos^{2}\theta}{(1 + \xi^{2})^{3/2}} \right] \right\} \tag{C1}$$

According to the procedure of reference 13, it is necessary to make a Fourier analysis of the three terms in the braces and then to insert the Fourier coefficients in equation (8) of reference 13.

In the first term in the braces, the expression in the brackets is the first and only Fourier coefficient. Changing ξ to β and inserting the expression into the inner integral of equation (8) of reference 13 gives

$$\lim_{\sigma \to 0} \int_{-\infty}^{\infty} \left(\frac{\beta \sigma}{\sqrt{1 + \beta^2 \sigma^2}} - \frac{\beta}{\sqrt{1 + \beta^2}} \right) \cos q(\beta - \xi) d\beta$$

which, if integrated by parts, reduces to

$$\lim_{\sigma \to 0} \frac{1}{q} \int_{-\infty}^{\infty} \left[\frac{1}{(1+\beta^2)^{3/2}} - \frac{\sigma}{(1+\beta^2\sigma^2)^{3/2}} \right] \sin q(\beta - \xi) d\beta$$

The contribution of the first term in the brackets is

$$\frac{1}{q} \int_{-\infty}^{\infty} \frac{\sin q(\beta - \xi) d\beta}{(1 + \beta^2)^{3/2}} = -2K_1(q) \sin q\xi$$

(See reference 15, p. 52.) The fact that the contribution of the second term in the brackets is zero follows immediately, upon performing the change of variable $p = \beta \sigma$, from the Riemann-Lebesgue lemma (reference 11, p. 172).

The third term in the braces of equation (C1) is converted as follows:

$$-\frac{\xi \sin \theta}{\xi^2 + \sin^2 \theta} \left[\frac{1}{\sqrt{1 + \xi^2}} - \frac{\cos^2 \theta}{(1 + \xi^2)^{3/2}} \right] = -\frac{\xi \sin \theta}{(1 + \xi^2)^{3/2}}$$

so that again the first and only Fourier coefficient is given directly. Inserting it into the inner integral of equation (8) of reference 13 and integrating by parts gives

$$-\int_{-\infty}^{\infty} \frac{\beta}{\left(1+\beta^2\right)^{3/2}} \cos q(\beta-\xi) d\beta = \int_{-\infty}^{\infty} \frac{q \sin q(\beta-\xi)}{\sqrt{1+\beta^2}} d\beta$$

The second term in the braces of equation (C1) is not a one-term Fourier series. Its nth Fourier coefficient is given by a constant times

$$\int_{0}^{2\pi} \frac{\xi \sin \theta \sin n\theta}{\sigma(\xi^{2} + \sin^{2}\theta)} \left(1 - \frac{1}{\sqrt{1 + \xi^{2}\sigma^{2}}}\right) d\theta$$

Inserting this expression in the inner integral of equation (8) of reference 13, and reversing the order of integration gives

$$\int_{0}^{2\pi} \sin \theta \sin n\theta \int_{-\infty}^{\infty} \frac{\beta}{\sigma(\beta^2 + \sin^2 \theta)} \left(1 - \frac{1}{\sqrt{1 + \beta^2 \sigma^2}}\right) \cos q(\beta - \xi) d\beta d\theta$$

After substitution of $p = \beta \sigma$, the limit of the inner integral becomes

$$\lim_{\sigma \longrightarrow 0} \frac{1}{\sigma} \int_{-\infty}^{\infty} \frac{p}{p^2 + \sigma^2 \sin^2 \theta} \left(1 - \frac{1}{\sqrt{1 + p^2}} \right) \cos q \left(\frac{p}{\sigma} - \xi \right) dp$$

Integration by parts and elimination of terms in σ^2 reduces this expression to

$$\lim_{\sigma \to 0} \frac{1}{q} \int_{-\infty}^{\infty} \left[\frac{1}{p^2} - \frac{2p^2 + 1}{p^2(1 + p^2)^{3/2}} \right] \sin q \left(\frac{p}{\sigma} - \xi \right) dp$$

which is zero, by the Riemann-Lebesgue lemma.

Finally, then, for the unit doublet $\left(\frac{\Gamma\sigma}{4\pi}=1\right)$

$$\Phi_{2} = \frac{2 \sin \theta}{\pi} \int_{0}^{\infty} \frac{J_{1}(iq\rho)}{iqJ_{1}(iq)} \left[qK_{0}(q) + K_{1}(q)\right] \sin q\xi \,dq$$

$$\frac{\partial \Phi_{2}}{\partial \xi}\Big|_{\rho=1} = \frac{2 \sin \theta}{\pi} \int_{0}^{\infty} \frac{J_{1}(iq)}{iJ_{1}(iq)} \left[qK_{0}(q) + K_{1}(q) \right] \cos q\xi \, dq$$

The potential Φ_0 of a unit doublet line along the axis is

$$\Phi_0 = \frac{\zeta}{\eta^2 + \zeta^2} \left(\frac{\xi}{\sqrt{\xi^2 + \eta^2 + \zeta^2}} + 1 \right) = \frac{\sin \theta}{\rho} \left(\frac{\xi}{\sqrt{\xi^2 + \rho^2}} + 1 \right)$$

whence

$$\frac{\partial \Phi_0}{\partial \xi}\Big|_{\rho=1} = \frac{\sin \theta}{(\xi^2 + 1)^{3/2}}$$

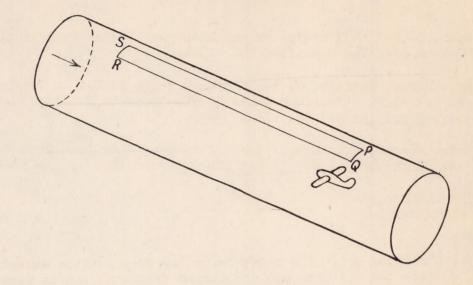
The flow of the usual reflection vortices for wings of finite span reduces, as the span becomes arbitrarily small, to a uniform upflow in the finite section of the tunnel and therefore contributes nothing to the longitudinal velocity.

The coefficient of $\sin \theta$ in $-\frac{\partial (\Phi_0 + \Phi_C)}{\partial \xi}\Big|_{\rho=1}$ is thus seen to be the expression given in equation (33).

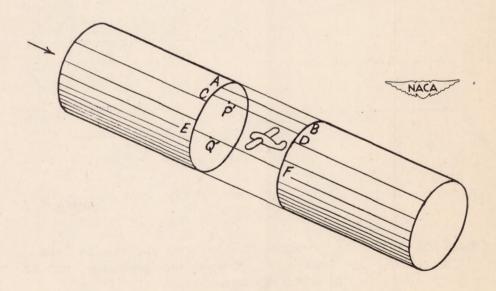
REFERENCES

- 1. Prandtl, L.: Theory of Lifting Surfaces. Part II. NACA IN No. 10, 1920.
- 2. Theodorsen, Theodore, and Silverstein, Abe: Experimental Verification of the Theory of Wind-Tunnel Boundary Interference. NACA Rep. No. 478, 1934.
- 3. Weinig, F.: Der Strahleinfluss bei offenen Windkanalen. Luftfahrtforschung, Bd. 13, Nr. 7, July 20, 1936, pp. 210-213.
- 4. Poggi, L.: Sulla variazione da apportarsi ai resultati delle esperienze eseguite al tunnel aerodinamico su di un modello alare. L'Aerotecnica, vol. XI, fasc. 4, April 1931, pp. 424-445.
- 5. Kúchemann, Dietrich, and Vandrey, Friedrich: Über den Einfluss der Düse (oder des Auffangtrichters) auf Widerstandsmessungen im Freistrahl. Z.f.a.M.M., Bd. 21, Nr. 1, Feb. 1941, pp. 17-31.
- 6. Vandrey, F.: Der Düseneinfluss auf die Windkanalkorrekturen bei ebener Strömung. Jahrb. 1942 der deutschen Luftfahrtforschung, R. Oldenbourg (Munich), pp. I 786-I 793.
- 7. Toussaint, A.: Experimental Methods Wind Tunnels. Influence of the Dimensions of the Air Stream. Vol. III of Aerodynamic Theory, div. I, part 1, ch. III, W. F. Durand, ed., Julius Springer (Berlin), 1935, p. 304.
- 8. Theodorsen, Theodore: The Theory of Wind-Tunnel Wall Interference. NACA Rep. No. 410, 1931.
- 9. Schliestett, George Van: Experimental Verification of Theodorsen's Theoretical Jet-Boundary Correction Factors. NACA IN No. 506, 1934.
- 10. Kellogg, Oliver Dimon: Foundations of Potential Theory. Julius Springer (Berlin), 1929, p. 373.
- 11. Whittaker, E. T., and Watson, G. N.: A Course of Modern Analysis. Fourth ed., Cambridge Univ. Press (London), 1927. (Reprinted 1940.)
- 12. Madelung, Erwin: Die Mathematischen Hilfsmittel des Physikers (Mathematical Tools for the Physicist). Dover Publications, 1943, p. 16.
- 13. Eisenstadt, Bertram J.: Boundary-Induced Upwash for Yawed and Swept-Back Wings in Closed Circular Wind Tunnels. NACA IN No. 1265, 1947.

- 14. Watson, G. N.: A Treatise on the Theory of Bessel Functions. Second ed., The Macmillan Co., 1944.
- 15. Gray, Andrew, Mathews, G. B., and MacRobert, T. M.: A Treatise on Bessel Functions and Their Applications to Physics. Second ed., Macmillan and Co., Ltd., 1931.
- 16. Jahnke, Eugene, and Emde, Fritz: Tables of Functions with Formulae and Curves. Rev. ed., Dover Publications (New York), 1943.
- 17. Milne-Thomson, L. M.: The Calculus of Finite Differences.
 Macmillan and Co., Ltd., 1933.

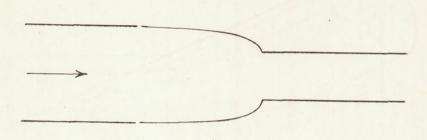


(a) Infinitely long open tunnel.

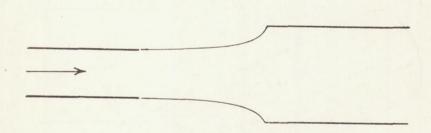


(b) Open jet between closed entrance and exit regions.

Figure 1.- Illustrations for discussion of surface perturbation velocity in open wind tunnels.



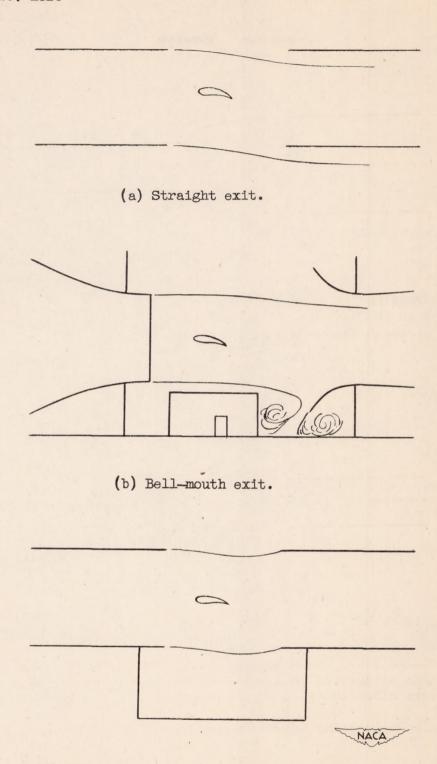
(a) Contracting jet. The pressure on the free surface exceeds both the upstream and downstream pressure, but is very close to the upstream pressure.



NACA

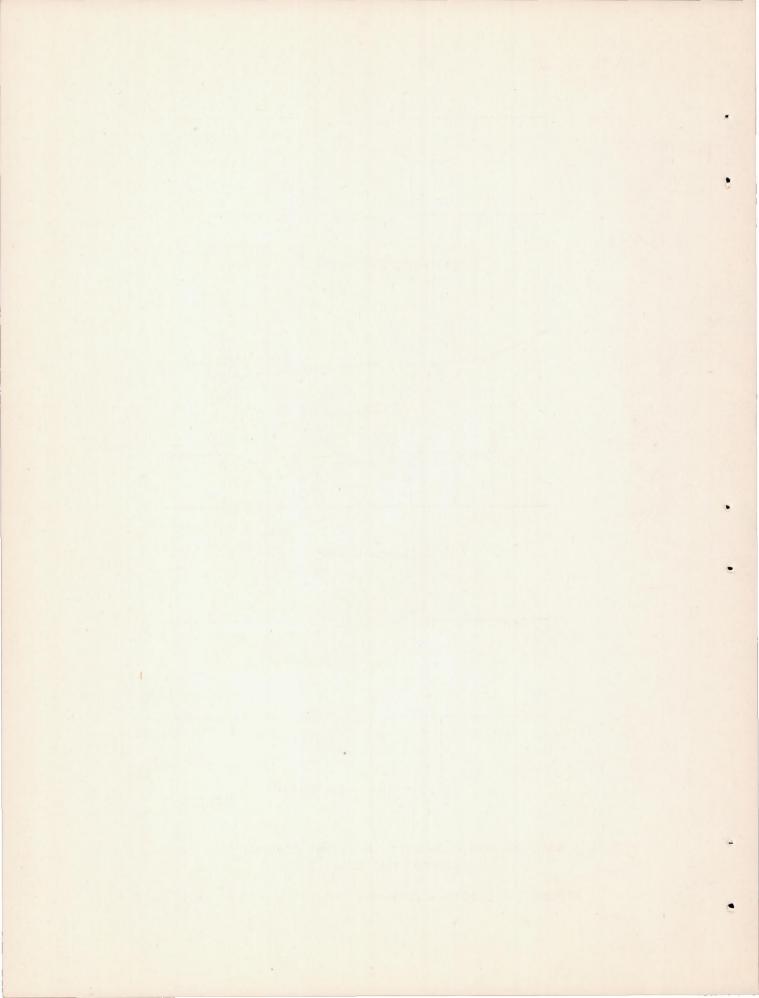
(b) Expanding jet. The pressure on the free surface is less than either the upstream or downstream pressure, but is very close to the upstream pressure.

Figure 2.- Contracting and expanding jets (2 or 3 dimensions).



(c) Enclosed space beneath the lower free surface (two-dimensional tunnel).

Figure 3.- Spillage from the lower lip of the exit.



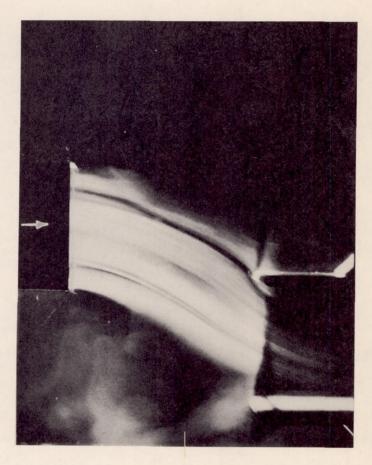
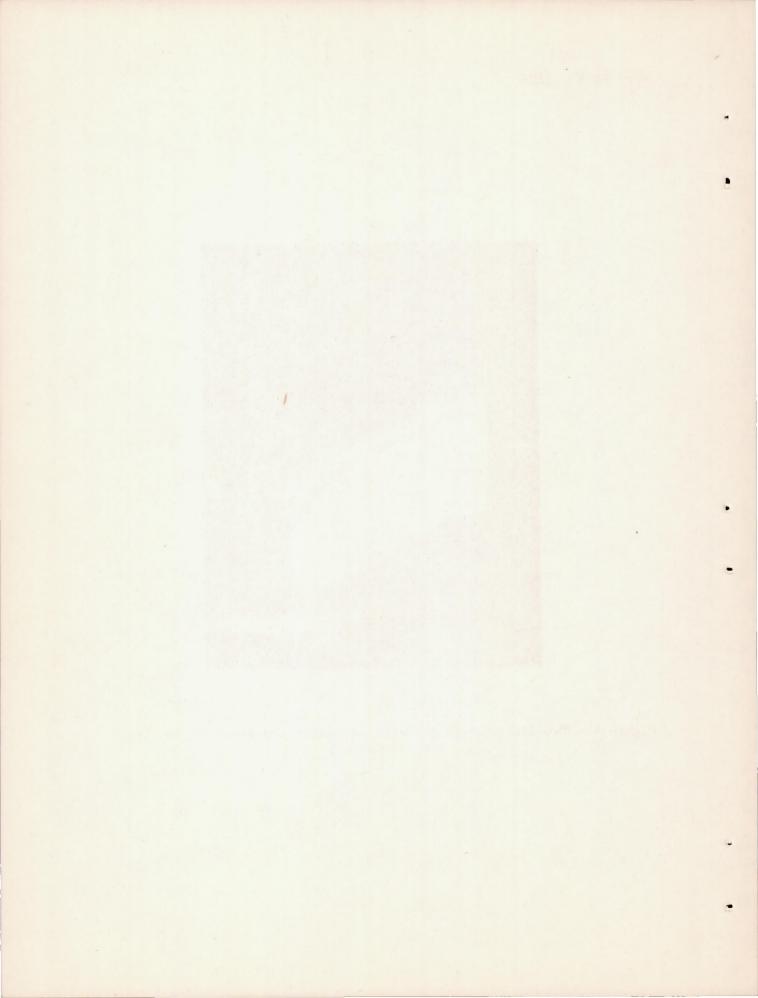
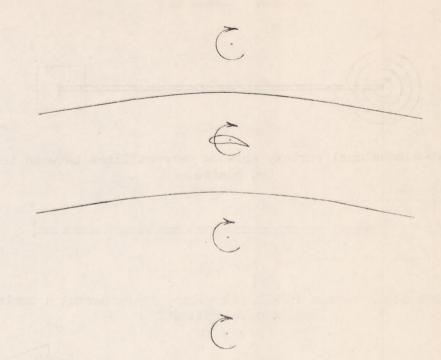
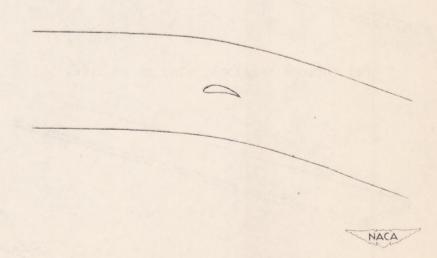


Figure 4.- Two-dimensional jet with different pressures on the two free surfaces.



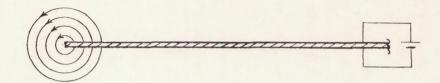


(a) Deformation due to image system; no downwash at the wing itself.

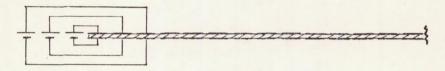


(b) Undeformed upstream flow; downwash at wing is half of that at infinity.

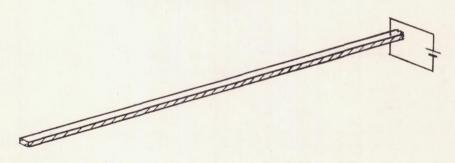
Figure 5.- Two-dimensional open tunnel of infinite length.



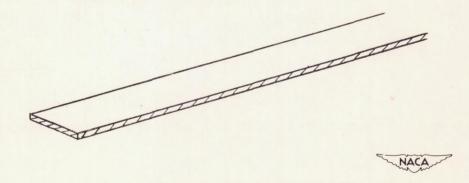
(a) Two-dimensional vortex, showing current lines between the two plates.



(b) Two-dimensional vortex in a perturbation field having a horizontal velocity component.

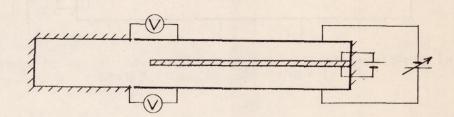


(c) Three-dimensional element of lift.

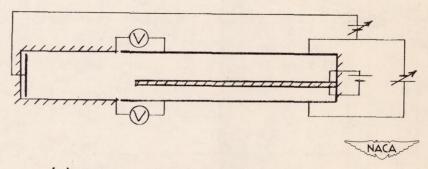


(d) Horseshoe vortex of finite span.

Figure 6.- Velocity-potential analogies for two- and three-dimensional lifting elements.

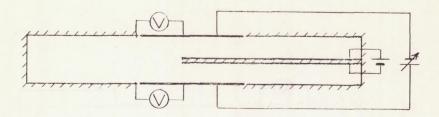


(a) Vortex on the center line.

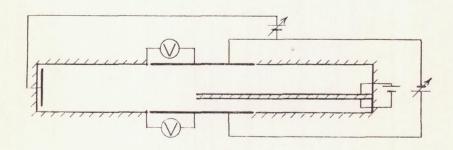


(b) Unsymmetrically located vortex.

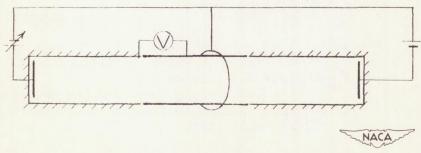
Figure 7.- Velocity-potential analogies for the two-dimensional closed-open tunnel.



(a) Vortex on the center line.

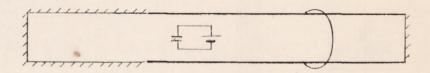


(b) Unsymmetrically located vortex (incomplete representation).

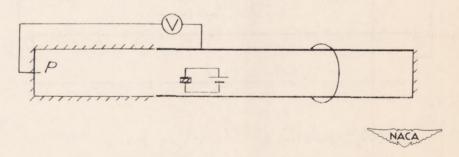


(c) Expanding or contracting jet.

Figure 8.- Velocity-potential analogies for the two-dimensional closedopen-closed tunnel.

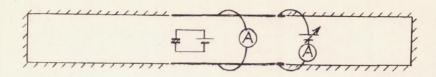


(a) Lifting element on the center line.

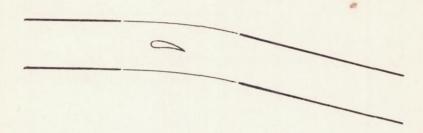


(b) Unsymmetrical location of the lifting element.

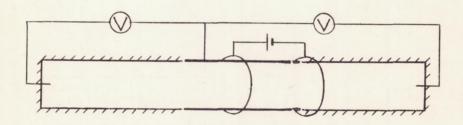
Figure 9.- Acceleration-potential analogies for the two-dimensional closed-open tunnel.



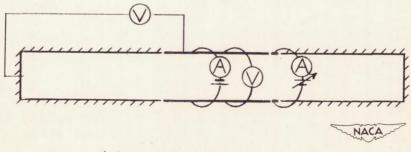
(a) Lifting element on the center line.



(b) Tunnel arrangement that corresponds to omitting the additional short strips.



(c) Expanding or contracting jet.



(d) Curving jet.

Figure 10.— Acceleration—potential analogies for the two-dimensional closed—open—closed tunnel.

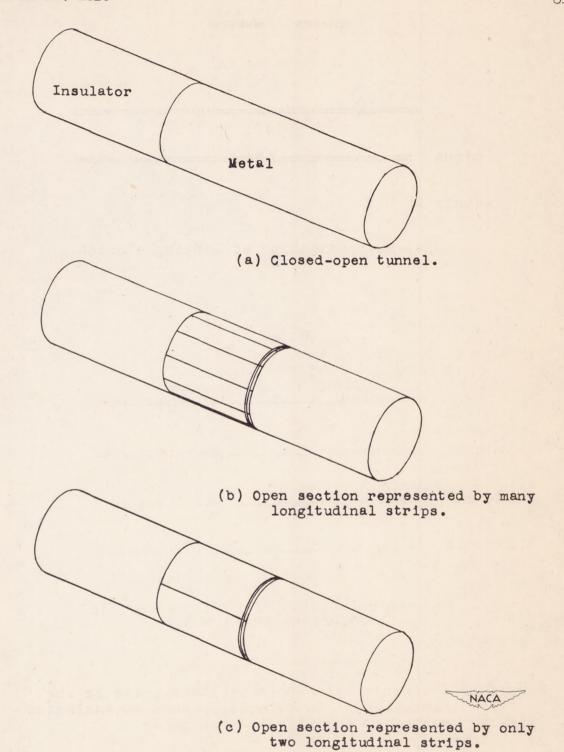
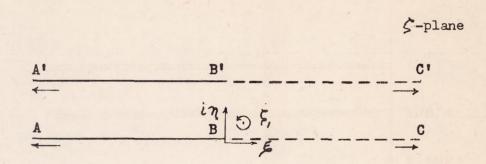


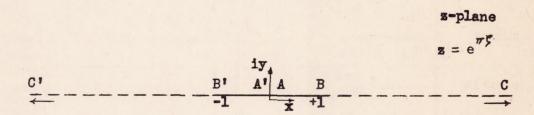
Figure 11.- Acceleration-potential analogy for three-dimensional closed-open tunnel and two approximate acceleration-potential analogies for three-dimensional closed-open-closed tunnels. The closed-open analogy may also be considered as an approximate analogy for the closed-open-closed tunnel.

				www.
minus	s communication	and the second		***************************************
equals	3 1990			
	(a) Representa	tion of	lifting	element.
	manning			
minus			uuuu	unumum.
quals		.,		Millill
equals				
			5	NACA
(1	closed-oper	on of or	en bound	lary in

Figure 12.- Acceleration-potential analogies as the difference between two velocity-potential analogies slightly shifted relative to each other.



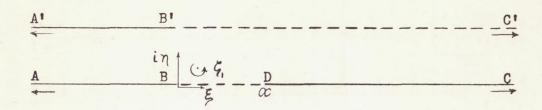
· 51



. Z1

Figure 13.— Physical and transformed spaces for two-dimensional closed-open tunnel of unit height.

5-plane

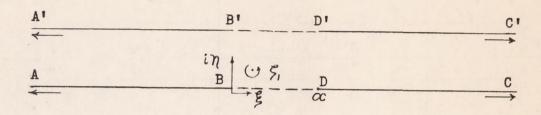


$$\mathbf{z} = \mathbf{e}^{\pi \mathbf{x}}$$

· z1

Figure 14.- Physical and transformed spaces for two-dimensional tunnel of unit height with one exit boundary.

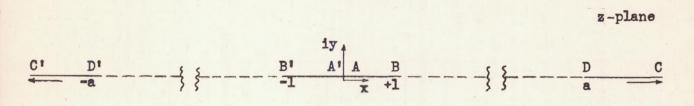
5 - plane

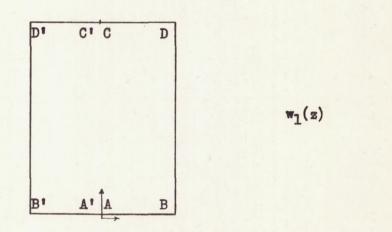




. z1

Figure 15.— Physical and transformed spaces for symmetrical two-dimensional closed—open—closed tunnel of unit height.





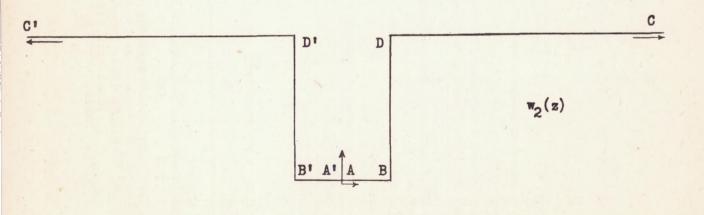


Figure 16.- Maps of the functions $w_1(z)$ and $w_2(z)$.

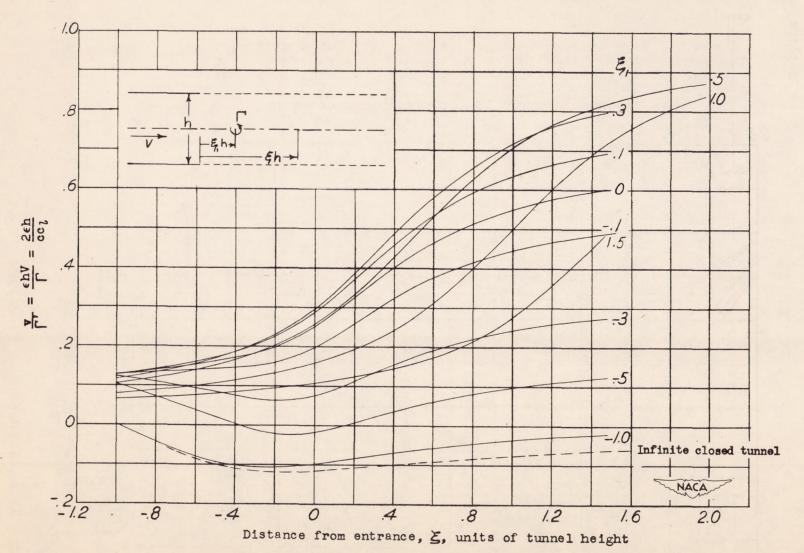


Figure 17.- Tunnel-induced angle on axis of two-dimensional closed-open tunnel, with vortex at several locations along axis.

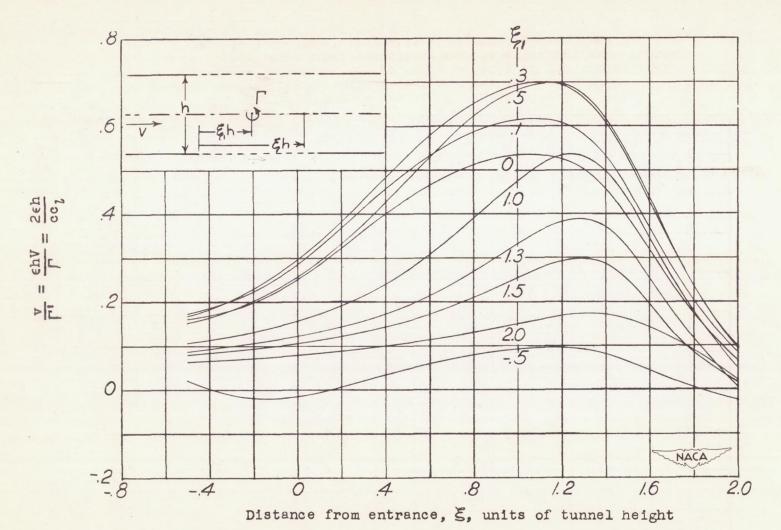


Figure 18.- Tunnel-induced angle on axis of symmetrical two-dimensional closed-open-closed tunnel, with vortex at several locations along axis. Length of open section is 1.5 times

tunnel height.

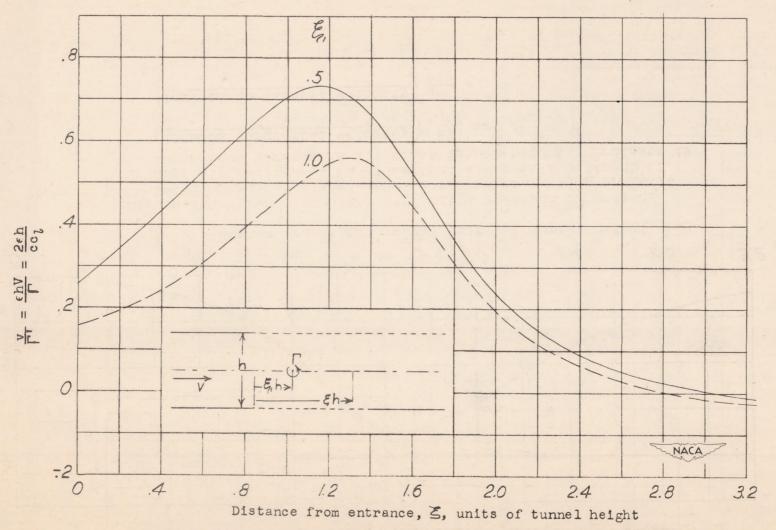
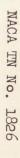


Figure 19.- Tunnel-induced angle on axis of two-dimensional closed-open-closed tunnel having one exit lip, with vortex at two locations along axis. Length of lower free surface is 1.5 times tunnel height.



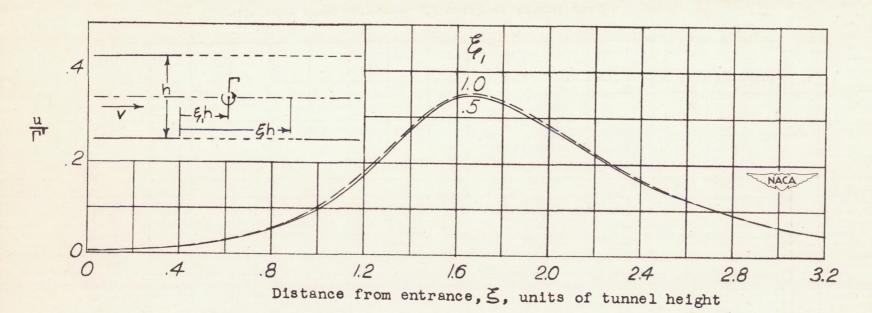


Figure 20.- Tunnel-induced horizontal velocity on axis of two-dimensional closed-open-closed tunnel having one exit lip, with vortex at two locations along axis. Length of lower free surface is 1.5 times tunnel height. Ordinate is
\[\left(\frac{\text{Induced horizontal velocity}}{V} \right) \frac{hV}{\Gamma}, \text{ or} \]
\[\left(\frac{\text{Induced horizontal velocity}}{V} \right) \frac{2h}{cc_1}. \]

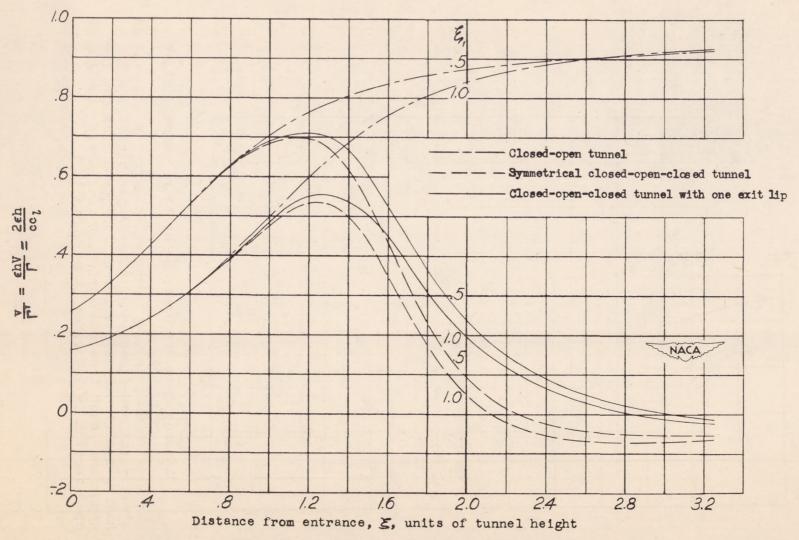
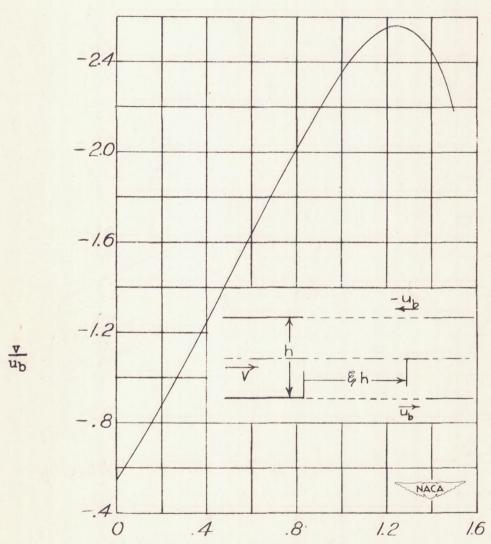


Figure 21.- Comparison of tunnel-induced angles on axis for three types of two-dimensional tunnels. Length of open sections for the closed-open-closed tunnels is 1.5 times tunnel height.



Distance from entrance, &, units of tunnel height

Figure 22.- Tunnel-induced vertical velocity v on axis of symmetrical two-dimensional closed-open-closed tunnel having additional velocities of -up and up on the upper and lower free boundaries, respectively. Length of open section is 1.5 times tunnel height.

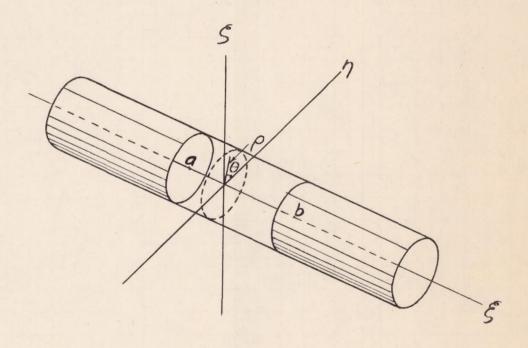
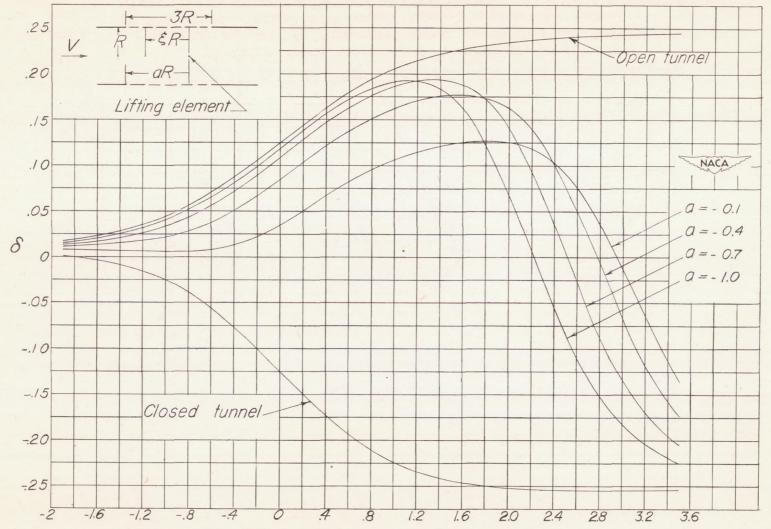
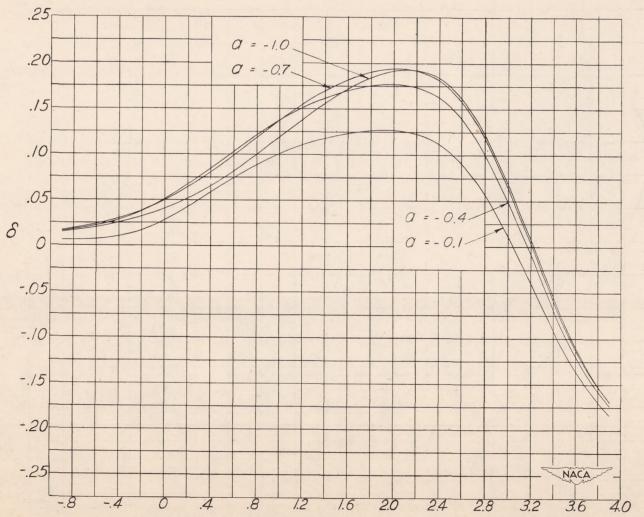


Figure 23-Closed - open-closed tunnel, showing coordinate systems.



Distance from lifting element, \$, units of tunnel radius
Figure 24.- Tunnel-induced velocity parameter along tunnel axis for several positions of the lifting element in a closed-open-closed circular tunnel.



Distance from entrance, \$-a, units of tunnel radius
Figure 25. - Tunnel-induced velocity parameter along tunnel axis for several positions
of the lifting element in a closed-open-closed circular tunnel.
(Same curves as on fig. 24, but plotted against distance from entrance.)

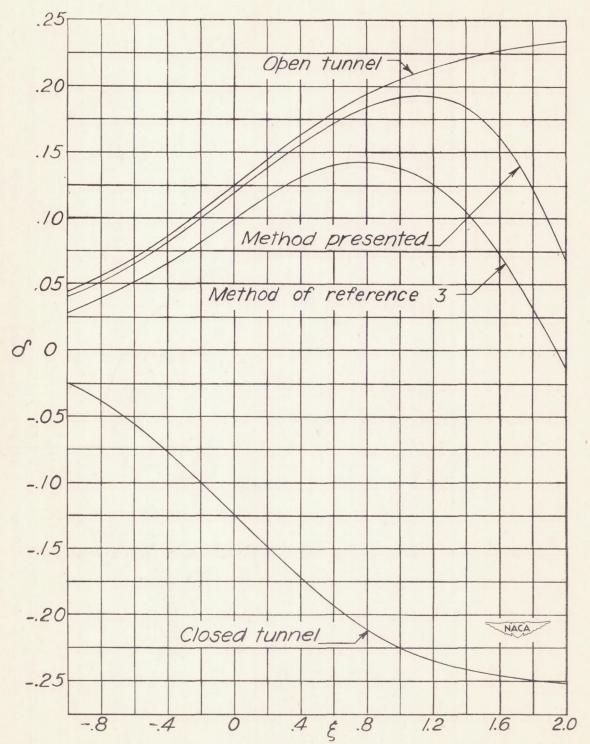


Figure 26.-Comparison of the results of the present paper with those of reference 3 for a=-1, together with those for open and closed circular tunnels.

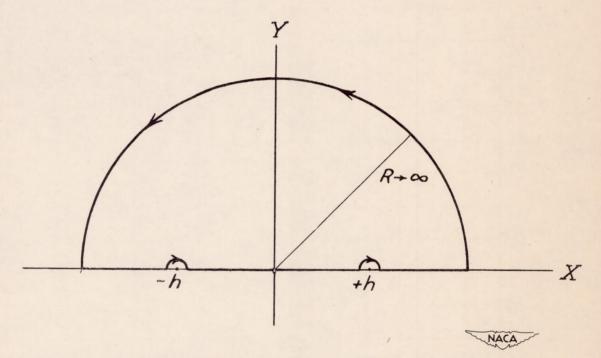


Figure 27.-Path of complex contour integration.